Response to Reviews for the ACPD paper "Organic peroxy radical chemistry in oxidation flow reactors and environmental chambers and their atmospheric relevance"

We thank the referees for their reviews. To facilitate the review process, we have copied the reviewer comments in black text. Our responses are in regular blue font. We have responded to all the referee comments and made alterations to our paper (**in bold text**). Figures, tables, and sections in the responses are numbered as in the *revised* manuscript unless otherwise specified, while page and line numbers refer to the ACPD paper.

Anonymous Referee #1

This paper follows a number of others reporting the characterisation and optimisation of operating conditions for oxidation flow reactors (OFRs) through both experimental and modeling studies. This work focuses on a model study of the fate of organic peroxy radicals within OFRs under different operating conditions and makes comparisons to the fates of such species in the atmosphere.

R1.0) While the rationale for such a study is sound, and the methods described are appropriate, the paper is quite long for the information it contains, and there are questions as to the wider interest and novelty of the work. It would help if the authors could state the main scientific outcomes and objectives of this work more clearly, and if some detail could be provided which outlines how assumptions regarding the fates of RO2 species have potentially impacted the results of previous studies.

We believe that our paper fulfills an important need for the rapidly growing and interdisciplinary OFR research community. The paper provides a critical assessment of best practices in the use of OFRs, and dispels common notions regarding the shortcomings of OFRs, and thus is useful. We have added the following text to the introduction (after L67 of the ACPD version) to clarify this matter:

"The use of oxidation flow reactors is growing rapidly in the atmospheric chemistry community. Some researchers have raised two concerns with regard to OFRs: (1) the chemical regime of OFRs may be unrealistic compared to the atmosphere and (2) OFRs are derivative of flow reactors with a long tradition in atmospheric chemistry, especially for chemical kinetic measurements, and thus there is not much new to be discussed or analyzed in their chemistry. While it is true that OFRs follow the tradition of flow tubes used in atmospheric chemistry, they attempt to simulate a much more complex system all-at-once and typically use much longer residence times, and thus many fundamental and practical issues arise that have not been addressed before. The need to achieve longer effective photochemical ages within a short residence time can, however, lead to

the occurrence of undesirable oxidation pathways. This paper uses computer modeling to define useful ranges in which to work."

Therefore, we strongly believe that the present paper does address the needs of people interested in practical OFR application and those interested in the study of fundamental chemical pathways). We do make a reasonable attempt to present the methods and results in a way that is both rigorous and accessible to many OFR users with limited chemical knowledge (e.g. researchers with more of an aerosol and/or engineering training), even though to knowledgeable chemists this paper might appear to be somewhat wordy and detail-oriented.

In the response to R1.8, we have modified some text in the ACPD paper to give more details on and highlight several features of RO_2 chemistry in the atmosphere and chambers.

See also the response to comment R1.12.

R1.1) Page 4, lines 117-122: Is production of RO2 from ozonolysis reactions or reactions between O(1D) and VOCs considered for conditions when significant ozone/O(1D) are present? Although photolysis of organics is considered, is there any consideration of photolysis of oxygenated VOCs (formaldehyde or acetaldehyde for example) which may photolyse to generate RO2 radicals?

While RO_2 production from ozonolysis and photolysis of VOCs and their reactions with $O(^1D)$ is possible in the OH OFRs that are the focus of this paper, these non-OH pathways are significant only when OH is suppressed or not sufficiently produced, i.e. under "risky" or "bad" conditions as defined in the paper. We have previously shown that all these non-OH reactions become important for similar reasons and photolysis at 254 nm is usually the most significant type of non-OH reactions (Peng et al., 2016). The physical conditions leading to significant 254 nm VOC photolysis (non-tropospheric chemistry) are of little experimental interest. Thus we do not believe that it is necessary to include RO_2 production through non-OH pathways in this study.

We have added the following text to the end of the paragraph between L117 and L125:

"**RO_2 production through other pathways, e.g. VOC ozonolysis and photolysis, is not considered, since all non-OH pathways of VOC destruction only become significant at low H_2O and/or high OHR_{ext} (Peng et al., 2016). These conditions lead to significant non-tropospheric VOC photolysis and thus are of little experimental interest.**"

R1.2) Page 4, lines 133-134: The authors assume average ambient HO2 concentrations of $1.5x10^8$ molecules cm-3 and kHO2+RO2 of 1.5x10-11 cm3 molecule-1 s-1. The generic rate coefficient for HO2 + RO2 used seems high, for HO2 + CH3O2 the rate coefficient is 5.2x10-12 cm3 molecule-1 s-1, while that for HO2 + C2H5O2 is 6.9x10-12 cm3 molecule-1 s-1. How do

the assumptions regarding [HO2] and kHO2+RO2 influence the results reported in this work? Similarly, how does the assumption regarding kRO2+NO influence the results?

In the typical OFR experiments focused on SOA formation that we are mainly studying in this paper, CH_3O_2 and $C_2H_5O_2$ are minor contributors to the total RO_2 pool. Their formation rates through methane and ethane oxidation are very small compared to the formation of larger RO_2 radicals from other VOCs. We thus do not believe that CH_3O_2 and $C_2H_5O_2$ are important intermediates of VOC oxidation that are able to significantly alter the overall OH, HO_2, and RO_2 budget in OFRs. In the ambient and chamber cases, OH and HO_2 have been prescribed. If CH_3O_2 and $C_2H_5O_2$ are not the RO_2 of interest (which is usually the case in SOA formation studies), the different rate constants of the reactions of CH_3O_2 and $C_2H_5O_2$ with HO_2 than the typical value used for RO_2+HO_2 in this study will have no impact on the results of the ambient and chamber cases.

For other unsubstituted and oxygenated RO_2 radicals, the rate constants of their reactions with HO_2 are indeed around 1.5×10^{-11} cm^3 $molecule^{-1}$ s^{-1} (~1–2 $\times10^{-11}$ cm^3 $molecule^{-1}$ s^{-1}; see Table 5 of Orlando and Tyndall, 2012). And the rate constants of RO_2+NO are indeed very close to 9×10^{-12} cm^3 $molecule^{-1}$ s^{-1} (see Table 1 of Orlando and Tyndall, 2012) for most RO_2 radicals, including CH_3O_2 and $C_2H_5O_2$. Only the rate constants of acyl RO_2+NO are ~x2 the value used in the paper.

For the modified text to clarify this issue, please refer to the response to comment R2.2.

R1.3) Page 4, line 152 (and elsewhere): Please consider changing ‘RO2s’ to ‘RO2 radicals’ or similar.

We have changed “RO_2s” to “RO_2 radicals” throughout the paper.

R1.4) Page 5, line 175: Please quantify the statement ‘acylperoxy nitrates barely decompose’ with an example.

We have modified the relevant sentences in L175–176 with some detail added to clarify this:

“**In OFRs operated at room temperature, acylperoxy nitrates barely decompose, as their thermal decomposition lifetime is typically ~1 h (Orlando and Tyndall, 2012), while OFR residence time is usually a few minutes. In contrast, peroxy nitrates of non-acyl RO_2 do decompose on a timescale of 0.1 s (Orlando and Tyndall, 2012).**”

R1.5) Page 6, line 205: What is the rationale for this production rate of OH? What is the VOC concentration used? (i.e. What is the pseudo-first-order rate coefficient?)

First, we would like to clarify that the text in L205 and below discusses OH loss rather than OH production. In this study, we use a proxy of external OH reactant (SO_2), but external OH reactivity (OHR_{ext}, the pseudo-first-order rate constant of OH loss due to external species (e.g. VOCs, CO, and SO_2)) is not constrained to one value. Instead, its effects are explored over a very wide range (1–1000 s^{-1}) across our model cases. The initial SO_2 concentration used in each model case is determined by the initial OHR_{ext} chosen for that case.

We use SO_2 as a surrogate of external OH reactants for simplicity. OHR_{ext} for VOCs evolves over time (upon oxidation of VOCs and the formation and later oxidation of the stable reaction products) (Nehr et al., 2014; Fuchs et al., 2017; Sato et al., 2017; Schwantes et al., 2017). This evolution plays an important role in OH loss over time, but is not well modeled even with explicit chemical scheme such as Master Chemical Mechanism (Sato et al., 2017; Schwantes et al., 2017). Using a slow-reacting external OH reactant, i.e. SO_2, as a proxy can roughly account for the relatively slow decay of OHR_{ext} (compared to that of primary VOCs) due to the generation of second and later generation products. As we already stated in the ACPD paper (L208–209), this rationale has been discussed in detail in our previous papers (Peng and Jimenez, 2017; Peng et al., 2018). As this paper is already long, we prefer not to extensively discuss this approximation in the text again.

Nevertheless, for more clarity, we have modified the text in L205 to read:

"**A generic slow-reacting VOC (with the same OH rate constant as SO_2) is used as the external OH reactant. Its initial concentration is determined by the initial OHR_{ext} in each model case. Then as this proxy external OH reactant slowly reacts, OHR_{ext} slowly decays. This slow change in OHR_{ext} represents not only the decay of the initial reactant but also the generation and consumption of later-generation products that continue to react with OH. The reason for this approximation has been discussed in detail in previous OFR modeling papers (Peng and Jimenez, 2017; Peng et al., 2018).**"

R1.6) Page 6, line 220 and page 10, line 370: Are the results from these simulations reported anywhere? How is this estimate achieved?

To address the Referee's question, we have modified text to L219 and L369 to include more details about these calculations. The modified text in L219 reads as follows:

"We used the fully chemically explicit (automated chemical mechanism generation based on available knowledge) box-model GECKO-A (Aumont et al., 2005) to simulate OH oxidation of several simple VOCs (e.g. propane and decane) under various OFR conditions with zero-NO. We consistently find that β~0.3."

And the modified text in L369:

"However, simulations using the GECKO-A model in urban (Mexico City) and forested (Rocky Mountains) atmospheres (Figure S8) show that acyl RO_2 can still be a major (very roughly 1/3) component of RO_2 at ages of several hours or higher.

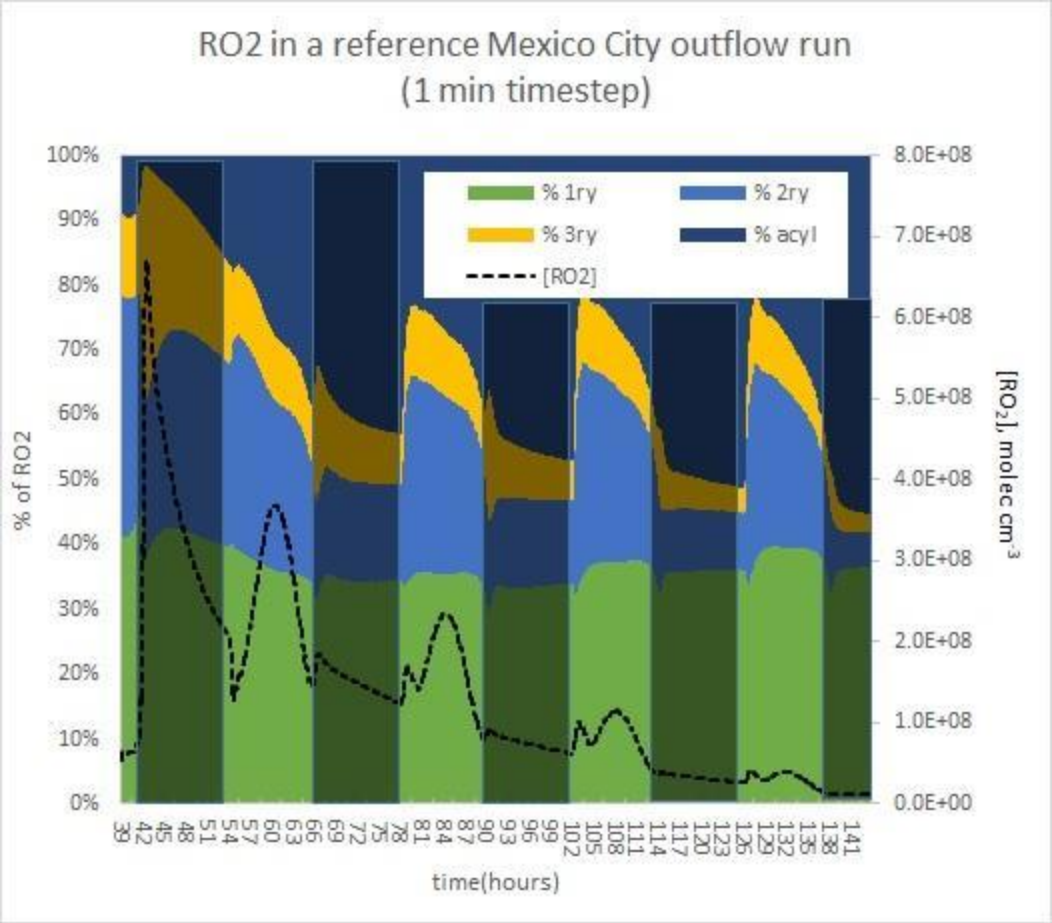

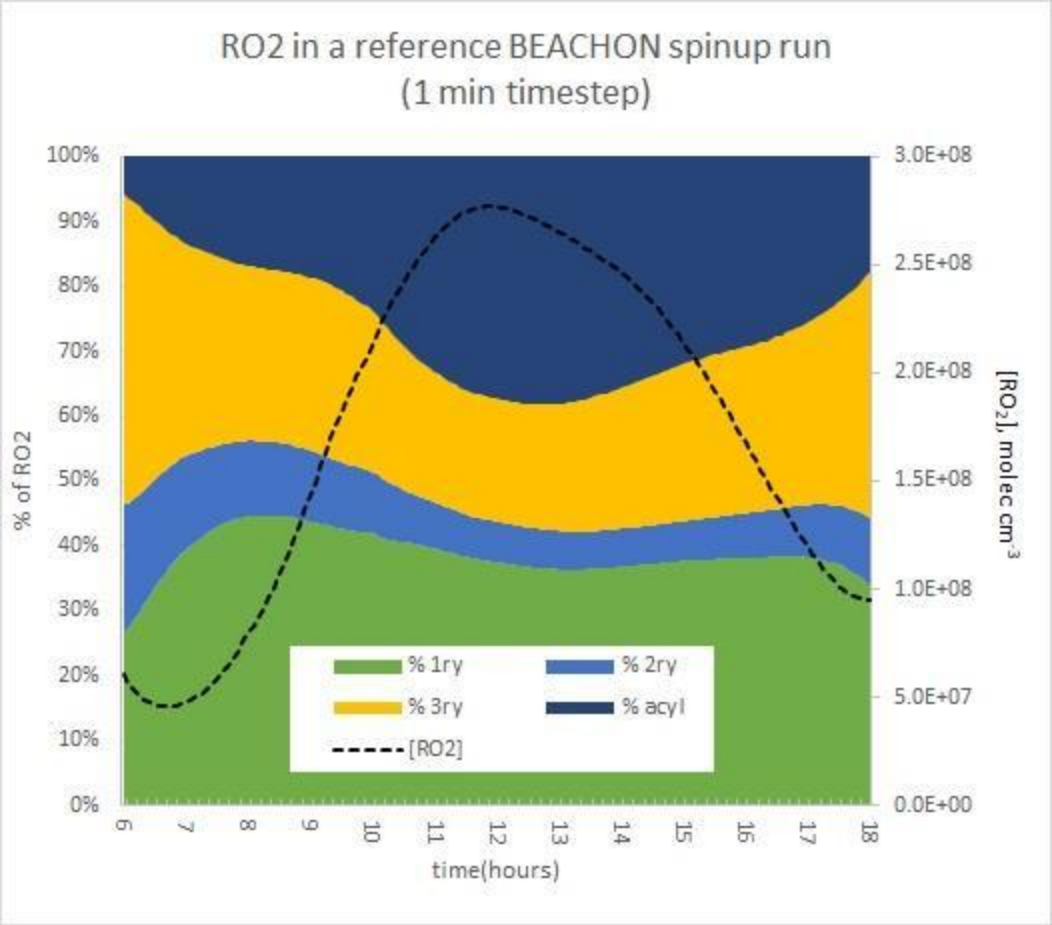

Figure S8. (a) RO_2 concentration and composition [primary (1ry), secondary (2ry), tertiary (3ry) and acyl RO_2] as a function of aging time for the simulation of a parcel of air advected from Mexico City during the MILAGRO 2006 campaign using the fully explicit GECKO-A model (Lee-Taylor et al., 2015). (b) The same for a GECKO-A simulation of air in a Rocky Mountain pine forest for the average diurnal cycle during the BEACHON-RoMBAS 2011 campaign (Palm et al., 2016; Hunter et al., 2017). Nighttime is denoted by shaded area."

R1.7) Page 8, line 304: I'm not sure forested areas should be described as 'low VOC' given high biogenic emissions in such regions.

For more clarity, we have modified the text to L303 to read:

"**Although OFRs can reasonably reproduce RO_2 fates in typical low- and moderate-OHR_{ext} ambient environments (e.g. typical pristine and forested areas; Figs. 1b,d and 3) and low-OHR_{ext} chambers, OFR185 cannot achieve relative importance of RO_2+RO_2 significantly larger than 50%, such as found in remote environments with higher VOC (e.g. P1 in Fig.**

1) and high-OHR_{ext} chamber experiments (e.g. C2 and C5 in Fig. 1; the distribution for C2 is also shown in Fig. 3)."

R1.8) Page 9, line 307: Are the labels C1, C2 etc. shown in the Figures described anywhere?

We have described the typical cases corresponding to these labels in Section 3.1.1 of the ACPD paper. Nevertheless, for added clarity we have modified the paragraph starting from L262 to include more discussion about the typical ambient and chamber cases:

"**In this case non-acyl RO_2 can have only three fates, i.e. RO_2+HO_2, RO_2+NO and RO_2+RO_2. The relative importance of these three fates can be shown in a triangle plot (Figure 1). The figure includes data points of OFR185 (including OFR185-iN_2O) and OFR254-70 (including OFR254-70-iN_2O), as well as several typical ambient and chamber studies, including two pristine remote area cases (P_1 and P_2) from the ATom-1 study (Wofsy et al., 2018), two forested area cases (F_1 and F_2) from the BEACHON-RoMBAS and GoAmazon campaigns, respectively (Ortega et al., 2014; Martin et al., 2016, 2017), an urban area case (U) from the CalNex-LA campaign (Ryerson et al., 2013) and five typical chamber experiment cases (C_1–C_5) from the FIXCIT study (Nguyen et al., 2014). These typical cases shown in Fig. 1 bring to light several interesting points:**

- **In all ambient and chamber cases, medium and slower RO_2+RO_2 contribute negligibly to the RO_2 fate. This confirms a common impression that self-/cross-reactions of many RO_2 radicals do not significantly affect RO_2 fates.**
- **However, if RO_2 self-/cross-reacts rapidly, RO_2+RO_2 can be the most important loss pathway among RO_2+RO_2, RO_2+HO_2 and RO_2+NO even in pristine regions with higher VOC (e.g. P_1 in Fig. 1) compared to an average pristine region case (P_2). Note that the P_1 case is still very clean compared to typical forested and urban areas (Table 2).**
- **Forested areas located in the same region as pollution sources are not as "low-NO" as one may expect (points F_1 and F_2 in Fig. 1). RO_2+NO contributes ~20–50% to RO_2 loss, as NO and HO_2 concentrations are on the same order of magnitude in these cases.**
- **RO_2+NO dominates over RO_2+RO_2 and RO_2+HO_2 in almost all urban areas. Even in relatively clean urban areas such as Los Angeles during CalNex-LA in 2010 (point U in Fig. 1), average NO is ~1 ppb, still sufficiently high to ensure the dominance of RO_2+NO among the three pathways.**
- **Various chamber cases in the FIXCIT campaign (low to high OHR_{ext}; low to high NO; points C_x in Fig. 1) are able to represent specific RO_2 fates that appear in different regions in the atmosphere.**

On these triangle plots, points for bad OFR conditions (in terms of non-tropospheric photolysis) are not shown because of the lack of experimental interest…"

R1.9) Page 12, line 421: Subscript in 'RO2'.

We have corrected it as suggested by the Referee.

R1.10) Page 13, line 490: Should this read 'Neither is the fast RO2 + RO2 …'?

We quote relevant sentences in that paragraph below:

"Since RO_2+HO_2 and RO_2+NO both can vary from negligible to dominant RO_2 fate in OFRs, chambers and the atmosphere (Figs. 1 and 2), these two pathways are not a concern in OFR atmospheric relevance considerations. Neither is the RO_2+RO_2 a major concern. Medium or slower RO_2+RO_2 is minor or negligible in the atmosphere and chambers, as well as in OFRs, as long as high OHR_{ext} is avoided in OFR254 (Fig. S2). Fast RO_2+RO_2 is somewhat less important in OFRs than in the atmosphere (Figs. 1b,d and 3), but is still qualitatively atmospherically relevant, given the uncertainties associated with the HO_x recycling ratios of various reactive systems and the huge variety of RO_2 types (and hence RO_2+RO_2 rate constants)."

We do not believe that the relevant text needs to be modified as suggested by the Referee, as the sentence "Neither is the RO_2+RO_2 a major concern" is followed by discussions on both medium/slower RO_2+RO_2 and fast RO_2+RO_2. Both types of RO_2+RO_2 are generally atmospherically relevant in OFRs.

R1.11) Page 16, line 585: Please provide a reference to the statement '. . . other major gas-phase radical reactions have weak or no temperature-dependence' or compare to a typical change in rate coefficient over a similar temperature range for RO2 + NO, RO2 + HO2 and RO2 + RO2.

We have added several examples and corresponding references into this sentence. The modified text now reads:

"**A 15 K temperature increase in OFRs would lead to RO_2 isomerization being accelerated by a factor of ~3, while other major gas-phase radical reactions have weak or no temperature-dependence (e.g. ~7%, ~5%, ~6% and ~19% slow-downs for isoprene+OH, toluene+OH, typical RO_2+NO and RO_2+HO_2, respectively; Atkinson and Arey, 2003; Ziemann and Atkinson, 2012).**"

R1.12) Page 16, lines 599-611: The utility of the RO2 fate estimator is unclear. What does it do above and beyond a simple yield/budget calculations requiring knowledge of [HO2], [RO2], [NO]

and the corresponding rate coefficients? It would be surprising if groups performing OFR studies, or similar, weren't already able to do such calculations.

Actually, we developed the RO_2 Fate Estimator partly due to a request by a well-known atmospheric chemist who is an expert in chamber experiments. While many chamber experimentalists are aware of the importance of RO_2 fate in their laboratory experiments, often analyses are presented that are not completely consistent with each other, or that do not include all the relevant pathways. We also found relatively few available datasets in the literature for chamber experiment RO_2 fate analysis, and we recommend performing such an analysis or reporting relevant data for it in the paper. Having a standardized RO_2 fate estimator available may facilitate some of these tasks.

For OFR users, their awareness of the importance of RO2 fate analysis may generally be lower than chamber experimentalists, as many of these groups have aerosol science or engineering backgrounds (e.g. aerosol optics and emission control of sources such as motor vehicles). As a result, RO_2 fate has rarely been reported in OFR studies. A user-friendly tool for these OFR practitioners to analyze this relatively complex problem would be very useful. Also quantities such as HO_2 concentration in OFRs are indeed very hard to measure, and many OFR users do not have tools to assess them independently. The estimation equations for these quantities embedded in the OFR RO_2 Fate Estimator makes realistic analyses of RO_2 fate in OFRs possible.

Therefore, we believe that both of our RO_2 Fate Estimators are of great practical interest and do not modify this paragraph (L599–611).

See also the response and added text in response to comment R1.1.

R1.13) Figure 1: The labels C1, P1, U etc. are unclear and/or overlapping with other labels on the plots.

We have modified all triangle plots to avoid overlap of the case labels. Below is an example (Figure 1a).

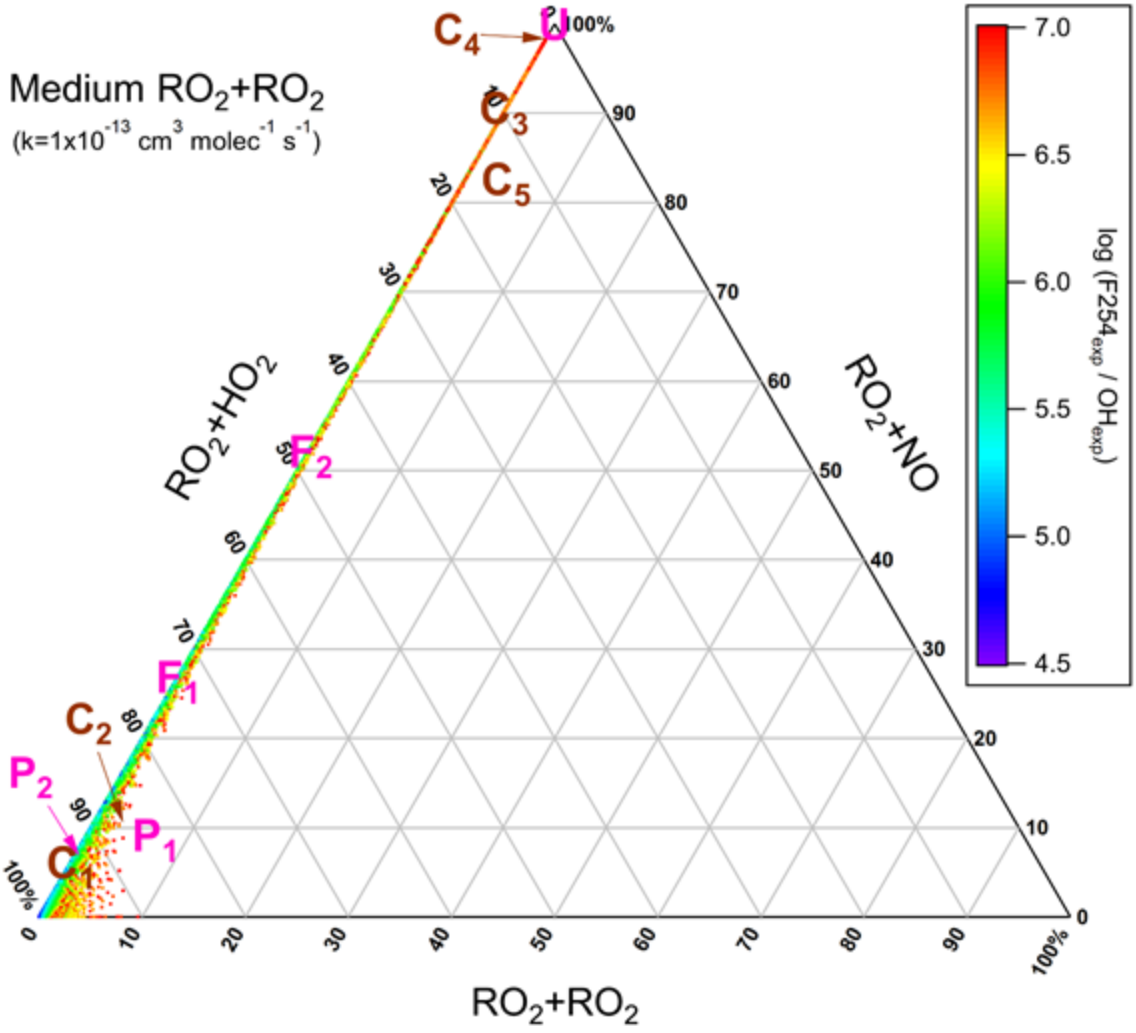

Anonymous Referee #2

This manuscript describes the use of a chemical model to evaluate the use of oxidative flow reactors. Overall, the work is important for groups using oxidative flow reactors, and includes a high quality analysis of the chemistry in those flow reactors, and should be published subject to appropriate revision. However, I have a few qualms that should be addressed by the authors, noted below.

R2.1) It is only a handful of groups that use OFRs, and the authors should address the generalizability of their research. Aside from acting as a handbook for OFR users, are there general notes on tropospheric chemistry that the authors can provide to the reader? For example, the relative importance of the different fates of RO2 is generally interesting, and a clear summarizing point from that first figure could be of use and generally interest.

We would like to clarify that OFRs are not only used by a handful groups. Currently there are ~50 research groups worldwide that use OFRs and this number is increasing very rapidly (probably by 10–15 groups per year). According to Google Scholar, the annual number of publications concerning OFRs has reached ~1/3 of that concerning traditional chambers and is increasing exponentially. We can comfortably claim that OFR has already become a mainstream atmospheric chemistry research tool. A study focused on such a tool, while comparing with the traditional tool (chambers) and the atmosphere, has enough scientific interest and practical importance to stand on its own.

Nevertheless, to address the Referee's concern, we have modified the text in Section 3.1.1 to provide more details of RO_2 fates in the troposphere and chambers. Please refer to the response to comment R1.8 for the modified text.

R2.2) The authors discuss RO2 as a general radical term, and in general their analysis makes sense from that perspective. However, in high NOx environments, RO2+NO dominantly produces RO+NO2, but sometimes produces organic nitrates (RONO2). The frequency of this branching will depend on the chemical identity of the RO2 precursor. I suspect this chemistry will impact the rates and radical balance in the OFR+N2O experiments. The authors include this reaction in Table 1, but do not discuss this reaction at all. Their model should be able to use RONO2 species to track the RO2 fate in high NOx experiments and see if the values are tropospherically relevant (i.e. will the OFR model - or OFR itself - produce a branching ratio that matches previous laboratory or field experiments?).

In the model, we focus on simulating generic RO_2 concentration and do not explicitly consider subsequent reactions of the products of RO_2 loss pathways. The overwhelming majority of NO_x in OFR-iN_2O exists in the form of NO_2 and NO_2 is dominantly produced from the oxidation of NO by O_3, HO_2 and OH (Peng et al., 2018), whose concentrations are orders of magnitude higher than corresponding ambient values. In the ACPD paper, we have already shown that RO_2 concentration in OFRs cannot be enhanced as much as O_3, HO_2 and OH. Therefore, whether a minor fraction of NO reacted with RO_2 produces NO_2 or not has virtually no impact on NO_2 concentration in OFR-iN_2O. Also, the HO_2 production from the reaction of RO with O_2 is already implicitly accounted for by the HO_x recycling described by β (see Section 2.3). In theory the $RONO_2$ formation branching ratio may affect β, but this impact should be small compared to the total HO_x recycling and generally negligible compared to the total HO_x production (Peng et al., 2015). As a result, subsequent reactions of the products of RO_2+NO and their branching ratios do not significantly affect the HO_x and NO_x balances in the simulations of OFR-iN_2O.

For simplicity, we do not specify the branching ratios of the $RO+NO_2$ and $RONO_2$ channels. As long as the relative contribution of RO_2+NO to the fate of RO_2 of interest in OFRs is close to that in other chamber or field experiments, the fractions (yields) of RO and $RONO_2$ in the total amount of the products of RO_2 loss pathways will also be close to those in other chamber or field experiments. Practically, readers can easily obtain those yields by multiplying the relative contribution of RO_2+NO by the branching ratios for RO_2 of interest.

For added clarity, we have modified the text to L145 to read:

"**Recommended general rate constants are available for RO_2+HO_2 and RO_2+NO (Ziemann and Atkinson, 2012; Table 1), albeit with some small dependencies on the type of RO_2 and a few deviations that are slightly larger but not important for the overall chemistry (e.g. CH_3O_2 and $C_2H_5O_2$ for RO_2+HO_2). We use these recommended values for generic RO_2 in this study. RO_2+NO has two main product channels, i.e. $RO+NO_2$ and $RONO_2$, whose branching ratios are RO_2-structure-dependent (Ziemann and Atkinson, 2012). We do not include these product channels in this study, since they have negligible impacts on the chemical scheme described here. This feature results from two facts: i) we focus on the generic RO_2 and do not explicitly consider the chemistry of products of the different RO_2 loss pathways; ii) the channel producing RO and NO_2 contributes little to NO_2 production (Peng et al., 2018).**"

R2.3) Finally, I would like to see the 'Guidelines for OFR Operation' either have a short bullet point summary of key points (or those in the Conclusions section), or be made more concise. Overall, it would behoove the authors to consider whether all the text and figures/tables are necessary to make their main points, or if there are additional places that could be removed. The paper is dense, which will reduce the readership. Reducing the number of acronyms (and making a table of whatever acronyms are left) would be very helpful for readability. There are so many 'OFR-subversions' that I had a challenging time reviewing portions of the manuscript.

We think that in Section 3.3 there is an obvious logical flow linking the points discussed, and hence prefer to make the bullet point summary in Section 4 (Conclusions) instead of Section 3.3. The modified second paragraph (starting from L630) now reads:

"**Besides the above-mentioned well-known pathways, RO_2+OH and RO_2 isomerization may also play an important role in RO_2 fate and sometimes result in atmospherically irrelevant RO_2 chemistry in OFRs. Here we summarize the main findings about all the pathways and the related guidelines for OFR operation:**

- **Under typical high-NO conditions, RO_2+NO dominates RO_2 fate and RO_2 lifetime is too short to allow most RO_2 isomerizations, regardless of whether in the atmosphere, chambers or OFRs, thus raising no concern about the atmospheric relevance of the OFR RO_2 chemistry.**

- **Under low-NO conditions, OFR254 cannot yield any physical conditions leading to sufficiently long RO_2 lifetime for its isomerization because of the high radical levels and their resilience to external perturbations in OFR254.**
- **In OFR185 with strong OH production (and hence high OH), RO_2+OH and RO_2 isomerization may strongly deviate from that in the atmosphere [becoming important and negligible, respectively, for relatively rapidly isomerizing RO_2 (rate constants on the order of 0.1 s^{-1})].**
- **To attain both atmospherically relevant VOC and RO_2 chemistries, OFR185 requires high H_2O, low UV and low OHR_{ext}. These conditions ensure minor or negligible RO_2+OH and a relative importance of RO_2 isomerization in RO_2 fate in OFRs within a factor of ~2 of that in the atmosphere.**
- **Under conditions allowing both VOC and RO_2 chemistries to be atmospherically relevant, the maximal photochemical age that can be reached is limited to a few eq. days. This age roughly covers the period required for maximum SOA formation in ambient air.**
- **To most realistically study much higher ages for SOA functionalization/fragmentation by heterogeneous oxidation, a sequence of low-UV SOA formation followed by a high UV condition (in the same reactor or in cascade reactors) may be needed.**
- **High H_2O, low UV and low OHR_{ext} in the OFR185-iNO mode can achieve conditions relevant to clean urban atmosphere, i.e. high-NO but not sufficiently high to inhibit common RO_2 isomerization.**"

In addition, we have added a glossary table as a part of the appendices to clarify the meanings of the different acronyms. Unfortunately, there are indeed multiple ways of running OFRs, each having very different chemical properties. Users have to choose a specific mode for a given experiment. The mode acronyms are thus necessary when discussing the different modes and their advantages and disadvantages:

"**Appendix A: Glossary of the acronyms (except field campaign names) used in the paper**

OFR	**oxidation flow reactor**
VOC	**volatile organic compound**
SOA	**secondary organic aerosol**
H_2O	**water vapor mixing ratio**
OHR_{ext}	**external OH reactivity (due to CO, SO_2, VOCs etc.)**
PAM	**Potential Aerosol Mass, a specific type of OFR**
OFR185	**oxidation flow reactor using both 185 and 254 nm light**

OFR254	**oxidation flow reactor using 254 nm light only**
OFR254-X	**OFR254 with X ppm O_3 initially injected**
OFR-iN_2O	**OFR with N_2O initially injected**
OFR185-iN_2O	**OFR185 with N_2O initially injected**
OFR254-iN_2O	**OFR254 with N_2O initially injected**
OFR254-X-iN_2O	**OFR254-X with N_2O initially injected**
OHR_{VOC}	**OH reactivity due to VOCs**
F185, F254 etc.	**UV photon flux at 185 nm, 254 nm etc.**
N_2O	**N_2O mixing ratio**
OH_{exp}, $F185_{exp}$ etc.	**exposure (integral over time) to OH, F185 etc.**

"

R2.4) line 51: remove the extra "(".

We have moved the second "(" in L51 as suggested by the Referee.

R2.5) line 212: I genuinely don't understand this sentence - please clarify (i.e. an accuracy of what?)

We have modified this sentence (in L212) for more clarity. Below is the modified sentence:

"**The outputs of our model (e.g. species concentrations and exposures) were estimated to be accurate to within a factor of 2–3 when compared with field OFR experiments; better agreement can generally be obtained for comparisons with laboratory OFR experiments (Li et al., 2015; Peng et al., 2015).**"

R2.6) line 352: Acyl RO2 +NO2 is typically referred to as an 'equilibrium', not 'quasi-irreversible reaction'. Consider what happens as temperature is increased - in the troposphere in summer, this equilibrium is important for most PAN-type compounds, and cannot be ignored! If this is the case in most OFRs, then there is a more serious problem with the RO2/NO2 and NO/NO2 ratios...

We do not think that a temperature increase of 10–20 K will significantly change the importance of acylperoxy nitrates in OFRs. The equilibrium constant of acyl RO_2+NO_2↔acyl RO_2NO_2 may change substantially. The O-N bond energy of acylperoxy nitrates is ~28 kcal/mol (Orlando and Tyndall, 2012), which we take as an approximate reaction energy of their decomposition. Then a 20 K temperature increase results in the equilibrium constant shifted toward RO_2+NO_2 by x~20. However, this shift is still too small relative to the equilibrium constant itself. For the generic acyl RO_2 in this study in an OFR at room temperature (298 K), RO_2+NO_2↔RO_2NO_2 has an equilibrium constant K_1=~$2x10^{-8}$ cm^3 $molecule^{-1}$. In a case with NO_2 of 10^{12} molecules cm^{-3} (a relatively low level in typical OFR-iN_2O experiments; Peng et al., 2018), we set K_2 = $K_1[NO_2]$ = $[RO_2NO_2]/[RO_2]$ = ~$2x10^4$ as the equilibrium constant for RO_2↔RO_2NO_2 (only when $[NO_2]$>>$[RO_2]$). Even if reduced by x20 by increasing temperature by 10 K, K_2 is still as high as ~1000, which means that only ~1 part per thousand of RO_2NO_2 will be present in the reactant form. Even if acylperoxy nitrate decomposition is x20 faster than at room temperature and the formed acyl RO_2 can irreversibly react with NO and decrease acylperoxy nitrate concentration, this effect is small: typically up to ~20% decrease in acylperoxy nitrate and usually negligible changes in NO and NO_2. The minor effect is due to i) acylperoxy concentration that is still very low, ii) NO concentration that is much lower than NO_2 and iii) acylperoxy nitrate decomposition lifetime that is still on the order of minutes.

We believe that it is appropriate to describe acyl RO_2+NO_2 in high-NO_x OFRs as a "quasi-irreversible" reaction *at room temperature* and add "**at room temperature**" after "the quasi-irreversible reaction RO_2+NO_2→RO_2NO_2" in L352 to be more rigorous.

For OFR conditions ~10–20 K higher than room temperature, since they are different than conditions in other reaction systems and that may be unclear to other researchers, we have included a summary of the discussion above in the paper. We have added the new text at the end of the paragraph starting from L583. The added text reads as follows:

"**Besides, reduction of acylperoxy nitrate formation in OFRs, which may be useful to mimic some urban environments where NO plays a larger role in acyl RO_2 fate (see Section 3.1.2), is unlikely to be achieved by increasing OFR temperature. The O-N bond energy of acylperoxy nitrates is ~28 kcal/mol (Orlando and Tyndall, 2012), which can be taken as an approximate reaction energy of their decomposition. Then a 20 K temperature increase results in the equilibrium constant of acyl RO_2+NO_2↔acyl RO_2NO_2 shifted toward RO_2+NO_2 by a factor of ~20. However, this shift is still too small relative to the equilibrium constant itself. It can be obtained by a simple calculation that for the generic acyl RO_2 in this study in an OFR at 318 K (20 K higher than room temperature) with NO_2 of 10^{12} molecules cm^{-3} (a relatively low level in typical OFR-iN_2O experiments; Peng et al., 2018), ~0.1% of the total amount of acyl RO_2 + acyl RO_2NO_2 will be present in the form of acyl RO_2. Even if acylperoxy nitrate decomposition is x20 faster than at room temperature and the formed acyl RO_2 can irreversibly react with NO and decrease acylperoxy nitrate concentration, this effect is small: typically up to ~20% decrease in acylperoxy nitrate and usually negligible changes in NO and NO_2. The minor effect is due to i) acylperoxy concentration that is still very low, ii) NO concentration that is much**

lower than NO_2 and iii) acylperoxy nitrate decomposition lifetime that is still on the order of minutes."

R2.7) line 361: what are typical NO/NO2 ratios in the OFR and in the troposphere? It would be helpful to summarize in a sentence.

We have modified the text to L361 to include the information requested by the Referee:

"**RO_2+NO_2 is an inevitable and dominant sink of most acyl RO_2 in high-NO_x OFRs, though the extent of this dominance differs substantially between the different OFR operation modes. In OFR254-70-iN_2O, RO_2+NO makes a minor or negligible contribution to acyl RO_2 fate because the required high O_3 very rapidly oxidizes NO to NO_2 and leads to very low NO-to-NO_2 ratios (e.g. ~0.003–0.03; see Fig. S7). In OFR185-iN_2O, the contribution of RO_2+NO can be somewhat significant, with typical NO-to-NO_2 of ~0.03–0.4. (Fig S7). Urban NO-to-NO_2 ratios vary widely, for example (roughly, and excluding significant tails in the frequency distributions), 0.02–1 for Barcelona, 0.007–0.7 for Los Angeles and Pittsburgh (see Fig. S7). Given these variations among different urban areas, RO_2+NO and RO_2+NO_2 for acyl RO_2 in OFR185-iN_2O can be regarded as relevant to urban atmospheres. Exceptions to the relevance of OFR185-iN_2O occur during morning rush hours (e.g. see the high NO-to-NO_2 tail for the Pittsburgh case in Fig. S7), near major NO sources, and/or in urban atmospheres with stronger NO emission intensity (e.g. Beijing, especially in winter; Fig. S7). In these cases, NO-to-NO_2 ratios may significantly exceed 1, and RO_2+NO may be the dominant acyl RO_2 loss pathway. Such high-NO conditions appear difficult to simulate in OFRs with the current range of techniques.**

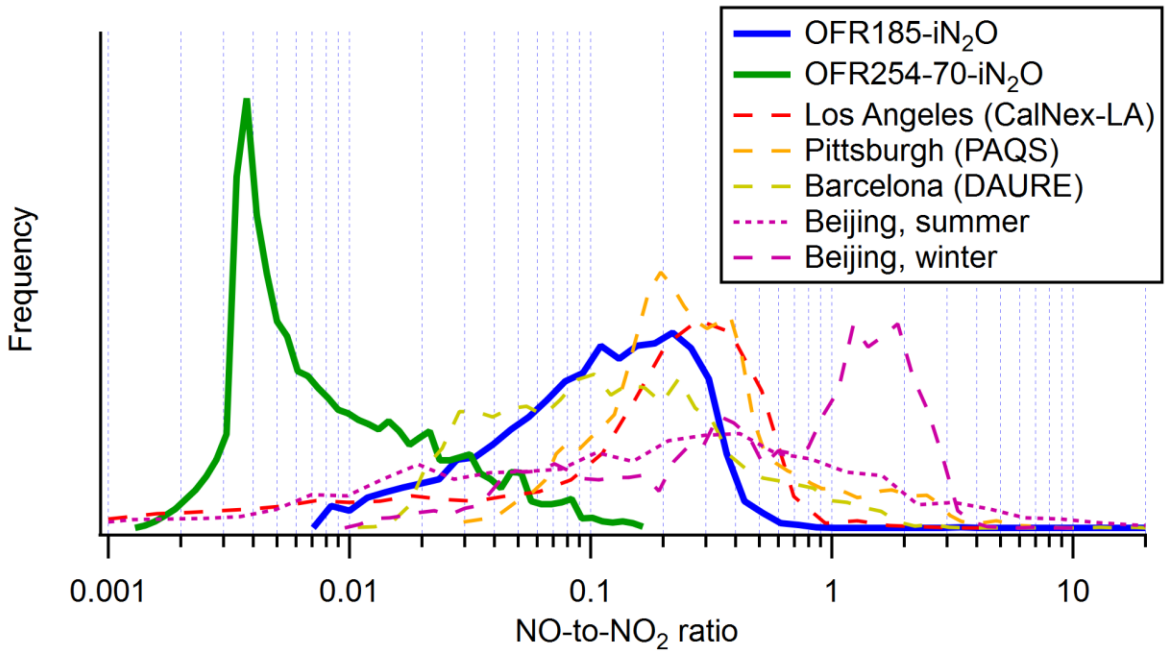

Figure S7. Frequency occurrence distributions of NO-to-NO_2 ratios for OFR185-iN_2O and OFR254-70-iN_2O model cases and measured at the Los Angeles, Pittsburgh and Barcelona ground sites during the CalNex-LA 2010, PAQS 2002 and DAURE 2009 campaigns, respectively (Zhang et al., 2005; Reche et al., 2011; Ryerson et al., 2013) and at a ground site in Beijing in both summer and winter (Hu et al., 2016). OFR cases under bad conditions are filtered out. The total areas of all distributions are identical."

R2.8) line 371: The sentence that states that acyl RO2 dominate aged air plumes requires a reference.

See the response to comment R1.6.

R2.9) line 432: 's' on the end of 'reaction(s)' should be deleted.

We have remove this "s" as suggested by the Referee.

Additional modification

We have discovered a bug in the OFR RO_2 Fate Estimator that affects the RO_2 fate estimation in OFR185 (low-NO mode) and fixed it in the revised Supplement.

References (for responses to both reviewers)

Atkinson, R. and Arey, J.: Atmospheric degradation of volatile organic compounds., Chem. Rev., 103(12), 4605–38, doi:10.1021/cr0206420, 2003.

Aumont, B., Szopa, S. and Madronich, S.: Modelling the evolution of organic carbon during its gas-phase tropospheric oxidation: development of an explicit model based on a self generating approach, Atmos. Chem. Phys., 5(9), 2497–2517, doi:10.5194/acp-5-2497-2005, 2005.

Fuchs, H., Novelli, A., Rolletter, M., Hofzumahaus, A., Pfannerstill, E. Y., Kessel, S., Edtbauer, A., Williams, J., Michoud, V., Dusanter, S., Locoge, N., Zannoni, N., Gros, V., Truong, F., Sarda-Esteve, R., Cryer, D. R., Brumby, C. A., Whalley, L. K., Stone, D., Seakins, P. W., Heard, D. E., Schoemaecker, C., Blocquet, M., Coudert, S., Batut, S., Fittschen, C., Thames, A. B., Brune, W. H., Ernest, C., Harder, H., Muller, J. B. A., Elste, T., Kubistin, D., Andres, S., Bohn, B., Hohaus, T., Holland, F., Li, X., Rohrer, F., Kiendler-Scharr, A., Tillmann, R., Wegener, R., Yu, Z., Zou, Q. and Wahner, A.: Comparison of OH reactivity measurements in the atmospheric

simulation chamber SAPHIR, Atmos. Meas. Tech., 10(10), 4023–4053, doi:10.5194/amt-10-4023-2017, 2017.

Hu, W., Hu, M., Hu, W., Jimenez, J. L., Yuan, B., Chen, W., Wang, M., Wu, Y., Chen, C., Wang, Z., Peng, J., Zeng, L. and Shao, M.: Chemical composition, sources, and aging process of submicron aerosols in Beijing: Contrast between summer and winter, J. Geophys. Res. Atmos., 121(4), 1955–1977, doi:10.1002/2015JD024020, 2016.

Huffman, J. A., Docherty, K. S., Aiken, A. C., Cubison, M. J., Ulbrich, I. M., DeCarlo, P. F., Sueper, D., Jayne, J. T., Worsnop, D. R., Ziemann, P. J. and Jimenez, J. L.: Chemically-resolved aerosol volatility measurements from two megacity field studies, Atmos. Chem. Phys., 9(1), 7161–7182, doi:doi:10.5194/acp-9-7161-2009, 2009.

Hunter, J. F., Day, D. A., Palm, B. B., Yatavelli, R. L. N., Chan, A. W. H., Kaser, L., Cappellin, L., Hayes, P. L., Cross, E. S., Carrasquillo, A. J., Campuzano-Jost, P., Stark, H., Zhao, Y., Hohaus, T., Smith, J. N., Hansel, A., Karl, T., Goldstein, A. H., Guenther, A., Worsnop, D. R., Thornton, J. A., Heald, C. L., Jimenez, J. L. and Kroll, J. H.: Comprehensive characterization of atmospheric organic carbon at a forested site, Nat. Geosci., 10(10), 748–753, doi:10.1038/NGEO3018, 2017.

Li, R., Palm, B. B., Ortega, A. M., Hu, W., Peng, Z., Day, D. A., Knote, C., Brune, W. H., de Gouw, J. and Jimenez, J. L.: Modeling the radical chemistry in an Oxidation Flow Reactor (OFR): radical formation and recycling, sensitivities, and OH exposure estimation equation, J. Phys. Chem. A, 119(19), 4418–4432, doi:10.1021/jp509534k, 2015.

Martin, S. T., Artaxo, P., Machado, L. A. T., Manzi, A. O., Souza, R. A. F., Schumacher, C., Wang, J., Andreae, M. O., Barbosa, H. M. J., Fan, J., Fisch, G., Goldstein, A. H., Guenther, A., Jimenez, J. L., Pöschl, U., Silva Dias, M. A., Smith, J. N. and Wendisch, M.: Introduction: Observations and Modeling of the Green Ocean Amazon (GoAmazon2014/5), Atmos. Chem. Phys., 16(8), 4785–4797, doi:10.5194/acp-16-4785-2016, 2016.

Martin, S. T., Artaxo, P., Machado, L., Manzi, A. O., Souza, R. A. F., Schumacher, C., Wang, J., Biscaro, T., Brito, J., Calheiros, A., Jardine, K., Medeiros, A., Portela, B., De Sá, S. S., Adachi, K., Aiken, A. C., Albl brecht, R., Alexander, L., Andreae, M. O., Barbosa, H. M. J., Buseck, P., Chand, D., Comstmstmstock, J. M., Day, D. A., Dubey, M., Fan, J., Faststst, J., Fisch, G., Fortner, E., Giangrande, S., Gilllles, M., Goldststein, A. H., Guenther, A., Hubbbbe, J., Jensen, M., Jimenez, J. L., Keutstsch, F. N., Kim, S., Kuang, C., Laskskin, A., McKinney, K., Mei, F., Millller, M., Nascimento, R., Pauliquevis, T., Pekour, M., Peres, J., Petäjä, T., Pöhlklker, C., Pöschl, U., Rizzo, L., Schmid, B., Shilllling, J. E., Silva Dias, M. A., Smith, J. N., Tomlmlinson, J. M., Tóta, J. and Wendisch, M.: The green ocean amazon experiment (GOAMAZON2014/5) observes pollution affecting gases, aerosols, clouds, and rainfall over the rain forest, Bull. Am. Meteorol. Soc., 98(5), 981–997, doi:10.1175/BAMS-D-15-00221.1, 2017.

Nault, B. A., Campuzano-Jost, P., Day, D. A., Schroder, J. C., Anderson, B., Beyersdorf, A. J., Blake, D. R., Brune, W. H., Choi, Y., Corr, C. A., de Gouw, J. A., Dibb, J., DiGangi, J. P., Diskin, G. S., Fried, A., Huey, L. G., Kim, M. J., Knote, C. J., Lamb, K. D., Lee, T., Park, T., Pusede, S. E., Scheuer, E., Thornhill, K. L., Woo, J.-H. and Jimenez, J. L.: Secondary Organic Aerosol Production from Local Emissions Dominates the Organic Aerosol Budget over Seoul, South Korea, during KORUS-AQ, Atmos. Chem. Phys. Discuss., 1–69, doi:10.5194/acp-2018-838, 2018.

Nehr, S., Bohn, B., Fuchs, H., Häseler, R., Hofzumahaus, A., Li, X., Rohrer, F., Tillmann, R. and Wahner, A.: Atmospheric photochemistry of aromatic hydrocarbons: OH budgets during SAPHIR chamber experiments, Atmos. Chem. Phys., 14(13), 6941–6952, doi:10.5194/acp-14-6941-2014, 2014.

Nguyen, T. B., Crounse, J. D., Schwantes, R. H., Teng, A. P., Bates, K. H., Zhang, X., St. Clair, J. M., Brune, W. H., Tyndall, G. S., Keutsch, F. N., Seinfeld, J. H. and Wennberg, P. O.: Overview of the Focused Isoprene eXperiment at the California Institute of Technology (FIXCIT): mechanistic chamber studies on the oxidation of biogenic compounds, Atmos. Chem. Phys., 14(24), 13531–13549, doi:10.5194/acp-14-13531-2014, 2014.

Orlando, J. J. and Tyndall, G. S.: Laboratory studies of organic peroxy radical chemistry: an overview with emphasis on recent issues of atmospheric significance, Chem. Soc. Rev., 41(19), 6294, doi:10.1039/c2cs35166h, 2012.

Ortega, J., Turnipseed, A., Guenther, A. B., Karl, T. G., Day, D. A., Gochis, D., Huffman, J. A., Prenni, A. J., Levin, E. J. T., Kreidenweis, S. M., DeMott, P. J., Tobo, Y., Patton, E. G., Hodzic, A., Cui, Y. Y., Harley, P. C., Hornbrook, R. S., Apel, E. C., Monson, R. K., Eller, A. S. D., Greenberg, J. P., Barth, M. C., Campuzano-Jost, P., Palm, B. B. B., Jimenez, J. L., Aiken, A. C., Dubey, M. K., Geron, C., Offenberg, J., Ryan, M. G., Fornwalt, P. J., Pryor, S. C., Keutsch, F. N., Digangi, J. P., Chan, A. W. H., Goldstein, A. H., Wolfe, G. M., Kim, S., Kaser, L., Schnitzhofer, R., Hansel, A., Cantrell, C. A., Mauldin, R. L. and Smith, J. N.: Overview of the Manitou experimental forest observatory: Site description and selected science results from 2008 to 2013, Atmos. Chem. Phys., 14(12), 6345–6367, doi:10.5194/acp-14-6345-2014, 2014.

Palm, B. B., Campuzano-Jost, P., Ortega, A. M., Day, D. A., Kaser, L., Jud, W., Karl, T., Hansel, A., Hunter, J. F., Cross, E. S., Kroll, J. H., Peng, Z., Brune, W. H. and Jimenez, J. L.: In situ secondary organic aerosol formation from ambient pine forest air using an oxidation flow reactor, Atmos. Chem. Phys., 16(5), 2943–2970, doi:10.5194/acp-16-2943-2016, 2016.

Peng, Z., Day, D. A., Ortega, A. M., Palm, B. B., Hu, W., Stark, H., Li, R., Tsigaridis, K., Brune, W. H. and Jimenez, J. L.: Non-OH chemistry in oxidation flow reactors for the study of atmospheric chemistry systematically examined by modeling, Atmos. Chem. Phys., 16(7), 4283–4305, doi:10.5194/acp-16-4283-2016, 2016.

Peng, Z., Day, D. A., Stark, H., Li, R., Lee-Taylor, J., Palm, B. B., Brune, W. H. and Jimenez, J. L.: HOx radical chemistry in oxidation flow reactors with low-pressure mercury lamps systematically examined by modeling, Atmos. Meas. Tech., 8(11), 4863–4890, doi:10.5194/amt-8-4863-2015, 2015.

Peng, Z. and Jimenez, J. L.: Modeling of the chemistry in oxidation flow reactors with high initial NO, Atmos. Chem. Phys., 17(19), 11991–12010, doi:10.5194/acp-17-11991-2017, 2017.

Peng, Z., Palm, B. B., Day, D. A., Talukdar, R. K., Hu, W., Lambe, A. T., Brune, W. H. and Jimenez, J. L.: Model Evaluation of New Techniques for Maintaining High-NO Conditions in Oxidation Flow Reactors for the Study of OH-Initiated Atmospheric Chemistry, ACS Earth Sp. Chem., 2(2), 72–86, doi:10.1021/acsearthspacechem.7b00070, 2018.

Praske, E., Otkjær, R. V., Crounse, J. D., Hethcox, J. C., Stoltz, B. M., Kjaergaard, H. G. and Wennberg, P. O.: Atmospheric autoxidation is increasingly important in urban and suburban North America, Proc. Natl. Acad. Sci., 115(1), 64–69, doi:10.1073/pnas.1715540115, 2018.

Reche, C., Viana, M., Moreno, T., Querol, X., Alastuey, A., Pey, J., Pandolfi, M., Prévôt, A., Mohr, C., Richard, A., Artiñano, B., Gomez-Moreno, F. J. and Cots, N.: Peculiarities in atmospheric particle number and size-resolved speciation in an urban area in the western Mediterranean: Results from the DAURE campaign, Atmos. Environ., 45(30), 5282–5293, doi:10.1016/j.atmosenv.2011.06.059, 2011.

Ryerson, T. B., Andrews, A. E., Angevine, W. M., Bates, T. S., Brock, C. A., Cairns, B., Cohen, R. C., Cooper, O. R., De Gouw, J. A., Fehsenfeld, F. C., Ferrare, R. A., Fischer, M. L., Flagan, R. C., Goldstein, A. H., Hair, J. W., Hardesty, R. M., Hostetler, C. A., Jimenez, J. L., Langford, A. O., McCauley, E., McKeen, S. A., Molina, L. T., Nenes, A., Oltmans, S. J., Parrish, D. D., Pederson, J. R., Pierce, R. B., Prather, K., Quinn, P. K., Seinfeld, J. H., Senff, C. J., Sorooshian, A., Stutz, J., Surratt, J. D., Trainer, M., Volkamer, R., Williams, E. J. and Wofsy, S. C.: The 2010 California Research at the Nexus of Air Quality and Climate Change (CalNex) field study, J. Geophys. Res. Atmos., 118(11), 5830–5866, doi:10.1002/jgrd.50331, 2013.

Sato, K., Nakashima, Y., Morino, Y., Imamura, T., Kurokawa, J. and Kajii, Y.: Total OH reactivity measurements for the OH-initiated oxidation of aromatic hydrocarbons in the presence of NO x, Atmos. Environ., 171, 272–278, doi:10.1016/j.atmosenv.2017.10.036, 2017.

Schwantes, R. H., Schilling, K. A., McVay, R. C., Lignell, H., Coggon, M. M., Zhang, X., Wennberg, P. O. and Seinfeld, J. H.: Formation of highly oxygenated low-volatility products from cresol oxidation, Atmos. Chem. Phys., 17(5), 3453–3474, doi:10.5194/acp-17-3453-2017, 2017.

Wofsy, S. C., Apel, E., Blake, D. R., Brock, C. A., Brune, W. H., Bui, T. P., Daube, B. C., Dibb, J. E., Diskin, G. S., Elkiins, J. W., Froyd, K., Hall, S. R., Hanisco, T. F., Huey, L. G., Jimenez, J. L., McKain, K., Montzka, S. A., Ryerson, T. B., Schwarz, J. P., Stephens, B. B., Weinzierl, B. and Wennberg, P.: ATom: Merged Atmospheric Chemistry, Trace Gases, and Aerosols, Oak Ridge, Tennessee, USA., 2018.

Zhang, Q., Canagaratna, M. R., Jayne, J. T., Worsnop, D. R. and Jimenez, J.-L.: Time- and size-resolved chemical composition of submicron particles in Pittsburgh: Implications for aerosol sources and processes, J. Geophys. Res., 110(D7), D07S09, doi:10.1029/2004JD004649, 2005.

Ziemann, P. J. and Atkinson, R.: Kinetics, products, and mechanisms of secondary organic aerosol formation, Chem. Soc. Rev., 41(19), 6582, doi:10.1039/c2cs35122f, 2012.

Organic peroxy radical chemistry in oxidation flow reactors and environmental chambers and their atmospheric relevance

Zhe Peng[1], Julia Lee-Taylor[1,2], John J. Orlando[2], Geoffrey S. Tyndall[2] and Jose L. Jimenez[1]

[1] Cooperative Institute for Research in Environmental Sciences and Department of Chemistry, University of Colorado, Boulder, Colorado 80309, USA
[2] Atmospheric Chemistry Observation and Modeling Laboratory, National Center for Atmospheric Research, Boulder, Colorado 80307, USA

Correspondence: Zhe Peng (zhe.peng@colorado.edu) and Jose L. Jimenez (jose.jimenez@colorado.edu)

Abstract. Oxidation flow reactors (OFR) are a promising complement to environmental chambers for investigating atmospheric oxidation processes and secondary aerosol formation. However, questions have been raised about how representative the chemistry within OFRs is of that in the troposphere. We investigate the fates of organic peroxy radicals (RO_2), which play a central role in atmospheric organic chemistry, in OFRs and environmental chambers by chemical kinetic modeling, and compare to a variety of ambient conditions to help define a range of atmospherically relevant OFR operating conditions. For most types of RO_2, their bimolecular fates in OFRs are mainly RO_2+HO_2 and RO_2+NO, similar to chambers and atmospheric studies. For substituted primary RO_2 and acyl RO_2, RO_2+RO_2 can make a significant contribution to the fate of RO_2 in OFRs, chambers and the atmosphere, but RO_2+RO_2 in OFRs is in general somewhat less important than in the atmosphere. At high NO, RO_2+NO dominates RO_2 fate in OFRs, as in the atmosphere. At high UV lamp setting in OFRs, RO_2+OH can be a major RO_2 fate and RO_2 isomerization can be negligible for common multifunctional RO_2, both of which deviate from common atmospheric conditions. In the OFR254 operation mode (where OH is generated only from photolysis of added O_3), we cannot identify any conditions that can simultaneously avoid significant organic photolysis at 254 nm and lead to RO_2 lifetimes long enough (~10 s) to allow atmospherically relevant RO_2 isomerization. In the OFR185 mode (where OH is generated from reactions initiated by 185 nm photons), high relative humidity, low UV intensity and low precursor concentrations are recommended for atmospherically relevant gas-phase chemistry of both stable species and RO_2. These conditions ensure minor or negligible RO_2+OH and a relative importance of RO_2 isomerization in RO_2 fate in OFRs within ~x2 of that in the atmosphere. Under these conditions, the photochemical age within OFR185 systems can reach a few equivalent days at most, encompassing the typical ages for maximum secondary organic aerosol (SOA) production. A small increase in OFR temperature may allow the relative importance of RO_2 isomerization to approach the ambient values. To study heterogeneous oxidation of SOA formed under atmospherically-relevant OFR conditions, a different UV source with higher intensity is needed after the SOA formation stage, which can be done with another reactor in series. Finally, we recommend evaluating the atmospheric relevance of RO_2 chemistry by always reporting measured and/or estimated OH, HO_2, NO, NO_2 and OH reactivity (or at least precursor composition and concentration) in all chamber and flow reactor experiments. An easy-to-use RO_2 fate estimator program is included with this paper to facilitate investigation of this topic in future studies.

1 Introduction

Laboratory reactors are needed to isolate and study atmospheric chemical systems. Environmental chambers have been a major atmospheric chemistry research tool for decades (Cocker et al., 2001; Carter et al., 2005; Presto et al., 2005; Wang et al., 2011; Platt et al., 2013). Over the last few years, oxidation flow reactors (OFRs, see Appendix A for the meanings of the acronyms) (Kang et al., 2007) have emerged as a promising complement to chambers, and are being used to investigate atmospheric oxidation processes, particularly volatile organic compound (VOC) oxidation and secondary organic aerosol (SOA) formation and aging (Kang et al., 2011; Lambe et al., 2015; Hu et al., 2016; Palm et al., 2016). These processes have air quality (Levy II, 1971), human health (Nel, 2005) and climate impacts (Stocker et al., 2014).

The most important advantage of OFRs is their ability to achieve relatively high photochemical ages (on the order of equivalent hours or days (assuming an average ambient OH concentration of 1.5×10^6 molecules cm^{-3}; Mao et al., 2009) in minutes instead of hours in chambers (Lambe et al., 2011). Rapid aging is usually achieved by highly active HO_x radical chemistry initiated by low-pressure Hg lamp emissions (185 and 254 nm) (Li et al., 2015; Peng et al., 2015). This allows shorter residence times in OFRs thus reducing the relative importance of gas and particle losses to walls (Palm et al., 2016), which can be very important in Teflon chambers (Cocker et al., 2001; Matsunaga and Ziemann, 2010; Zhang et al., 2014; Krechmer et al., 2016). In addition, lower costs and small size (volumes of the order of 10 L) of OFRs allow better portability. These, together with the ability to rapidly achieve high photochemical ages, are advantageous for field applications.

These advantages of OFRs have led a number of atmospheric chemistry research groups (Lambe and Jimenez, 2018) to deploy them in field (Hu et al., 2016; Ortega et al., 2016; Palm et al., 2016, 2017), source (Ortega et al., 2013; Tkacik et al., 2014; Karjalainen et al., 2016; Link et al., 2016) and laboratory studies (Kang et al., 2011; Lambe et al., 2013; Richards-Henderson et al., 2016; Lim et al., 2017).

~~However, the atmospheric relevance of VOC oxidation and SOA formation simulated in OFRs has repeatedly been called into question, because the UV wavelengths most commonly used to initiate OFR chemistry do not exist in the troposphere, and because OH levels in OFRs (10^8–10^{10} molecules cm^{-3}) can be much higher than tropospheric levels (10^6–10^7 molecules cm^{-3}; Mao et al., 2009; Stone et al., 2012).~~ While the use of oxidation flow reactors is growing rapidly in the atmospheric chemistry community, some researchers have raised two concerns with regard to OFRs: (1) the chemical regime of OFRs may be unrealistic compared to the atmosphere and (2) OFRs are derivative of flow reactors with a long tradition in atmospheric chemistry, especially for chemical kinetic measurements, and thus there is not much new to be discussed or analyzed in their chemistry. While it is true that OFRs follow the tradition of flow tubes used in atmospheric chemistry, they attempt to simulate a much more complex system all-at-once and typically use much longer residence times, and thus many fundamental and practical issues arise that have not been addressed before. The need to achieve longer effective photochemical ages within a short residence time can, however, lead to the occurrence of undesirable oxidation pathways.

To clarify this issue, a series of chemical kinetic modeling studies have been performed: Li et al. (2015) and Peng et al. (2015) established a radical chemistry and oxidation model whose predictions compare well against laboratory experiments and found that OH can be substantially suppressed by external OH reactants (e.g. SO_2, NO_x and VOCs externally introduced into the reactor); Peng et al. (2016) identified low water mixing ratio (H_2O) and/or high external OH reactivity (OHR_{ext}, i.e. first-order OH loss rate constant contributed by external OH reactants) as conditions that can cause significant non-tropospheric VOC reactions (e.g. through photolysis at 185 and/or 254 nm); Peng and Jimenez (2017) studied NO_y chemistry in OFRs and showed that high-NO conditions, where organic peroxy radicals react more rapidly with NO than with HO_2, can only be realized by simple NO injection in a very narrow range of physical conditions, whose application to investigating intermediate- and high-NO environments (e.g. urban area) is limited; Peng et al. (2018) thus evaluated a few new techniques to maintain high-NO conditions in OFRs and found injection of percent-level N_2O effective to achieve this goal.

While HO_x and NO_y chemistries have been extensively characterized in OFRs so far, organic peroxy radical (RO_2) chemistry has yet to be considered in detail, as previous studies have only considered the balance between RO_2+NO vs RO_2+HO_2. There has been some speculation that due to high OH concentrations in OFRs, RO_2 concentration and lifetime might be significantly different from ambient values, leading to dominance of RO_2 self/cross reactions and elimination of RO_2 isomerization pathways (Crounse et al., 2013; Praske et al., 2018). Given the central role RO_2 plays in atmospheric chemistry (Orlando and Tyndall, 2012; Ziemann and Atkinson, 2012) and the rapidly increasing use of OFRs, RO_2 chemistry in OFRs needs to be studied in detail to characterize the similarities and differences between their reactions conditions and those in the ambient atmosphere and traditional atmospheric reaction chambers.

In this paper, we address this need via modeling. All major known fates of RO_2 in OFRs will be investigated and compared with those in typical chamber cases and in the atmosphere. This comparison will provide insights into the atmospheric relevance of RO_2 chemistry in atmospheric simulation reactors and allow the selection of experimental conditions with atmospherically relevant RO_2 chemistry in experimental planning.

2 Methods

Due to a variety of loss pathways of RO_2 and a myriad of RO_2 types, RO_2 chemistry is of enormous complexity. We detail the RO_2 production and loss pathways of interest in this study, the approximations used to simplify this complex problem, and steps to investigate it methodically. We briefly introduce the base OFR design and the model, which are described in detail elsewhere (Kang et al., 2007; Peng et al., 2015, 2018).

2.1 Potential Aerosol Mass oxidation flow reactor (PAM OFR)

The concept of the base OFR design simulated in this study, the Potential Aerosol Mass (PAM) reactor, was first introduced by Kang et al. (2007) The geometry of the most popular PAM OFR is a cylinder of ~13 L volume. The PAM reactor we simulate is equipped with low-pressure Hg lamps (model no. 82-9304-03, BHK Inc.) emitting UV light at 185 and 254 nm. When both 185 and 254 nm photons

are used to generate OH (termed "OFR185"), water vapor photolysis at 185 nm produces OH and HO_2. Recombination of O_2 and $O(^3P)$, formed by O_2 photolysis at 185 nm, generates O_3. $O(^1D)$, formed through O_3 photolysis at 254 nm, reacts with water vapor and produces additional OH. 185 nm photons can be filtered by installing quartz sleeves around the lamps. This converts the reactor into "OFR254" mode, where photolysis of O_3, which must be initially injected, is the only OH production route. The notation "OFR254-X" is used to specify the initial amount of injected O_3 (X ppm) in OFR254. Lambe et al. (2017) and Peng et al. (2018) have shown that initial injection of N_2O is able to maintain up to tens of ppb NO in both OFR185 and OFR254. These modes are denoted "OFR185-iN_2O" and "OFR254-X-iN_2O", or more generally "OFR-iN_2O". In OFR254-iN_2O, $O(^1D)$ generated from O_3 photolysis reacts with N_2O to generate NO, while in OFR185-iN_2O, $O(^1D)$ is mainly supplied by N_2O photolysis at 185 nm (Peng et al., 2018).

2.2 RO_2 production and loss pathways

A single generic RO_2 is adopted for modeling purposes, to avoid the huge number of RO_2 types that would complicate effective modeling and analysis. In OH-initiated VOC oxidation, RO_2 is primarily produced via VOC+OH → R (+H_2O) followed by R+O_2 → RO_2, where R is hydrocarbyl or oxygenated hydrocarbyl radical. Since the second step is extremely fast in air (Atkinson and Arey, 2003), the first step controls the RO_2 production rate, which depends on OH concentration and OHR_{ext} due to VOCs (OHR_{VOC}, see Appendix ~~A~~ B for details). OHR_{VOC} also includes the contribution from oxidation intermediates of primary VOCs (e.g. methyl vinyl ketone and pinonic acid). When the information about oxidation intermediates is insufficient to calculate OHR_{VOC}, OHR due to primary VOCs is used instead as an approximant. RO_2 production through other pathways, e.g. VOC ozonolysis and photolysis, is not considered, since all non-OH pathways of VOC destruction only become significant at low H_2O and/or high OHR_{ext} (Peng et al., 2016). These conditions lead to significant non-tropospheric VOC photolysis and thus are of little experimental interest.

Table 1 lists all known RO_2 loss pathways. Among those, RO_2 photolysis, RO_2+NO_3 and RO_2+O_3 are not included in this study, since they are minor or negligible in OH-dominated atmospheres, chambers and OFRs for the following reasons.

- The first-order RO_2 photolysis rate constant is of the order of 10^{-2} s^{-1} at the highest lamp setting in OFRs (Kalafut-Pettibone et al., 2013) and of the order of 10^{-5} s^{-1} in the troposphere under the assumption of unity quantum yield (Klems et al., 2015), while RO_2 reacts with HO_2 at >1 s^{-1} at the highest lamp setting in OFRs and at ~2×10^{-3} s^{-1} in the troposphere. Note that in this study we assume an average ambient HO_2 concentration of 1.5×10^8 molecules cm^{-3} (Mao et al., 2009; Stone et al., 2012) and RO_2+HO_2 rate constant of 1.5×10^{-11} cm^3 $molecule^{-1}$ s^{-1} (Orlando and Tyndall, 2012).
- When daytime photochemistry is active, NO_3 is negligible in the atmosphere. In OFR-iN_2O modes, RO_2+NO_3 is negligible unless at very low H_2O and high UV intensity (abbr. UV hereafter), which result in high O_3 to oxidize NO_2 to NO_3 and keep HO_2 minimized. However, very low H_2O causes serious non-tropospheric organic photolysis (Peng et al., 2016) and thus these conditions are of no experimental interest.
- In the atmosphere RO_2+O_3 is thought to play some role only at night (Orlando and Tyndall, 2012).

Similar conditions may exist in some OFR254 cases, if a very large amount of O_3 is injected and H_2O and UV are kept very low to limit HO_x production. These conditions are obviously not OH-dominated and not further investigated in this study.

Of the RO_2 fates considered in this study, RO_2+HO_2 and RO_2+NO and RO_2+RO_2 have long been known to play a role in the atmosphere (Orlando and Tyndall, 2012). Recommended general rate constants are available for RO_2+HO_2 and RO_2+NO (Ziemann and Atkinson, 2012~~)~~; Table 1), albeit with some small dependencies on the type of RO_2 and a few deviations that are slightly larger but not important for the overall chemistry (e.g. CH_3O_2 and $C_2H_5O_2$ for RO_2+HO_2). We use these recommended values for generic RO_2 in this study. RO_2+NO has two main product channels, i.e. RO+NO_2 and $RONO_2$, whose branching ratios are RO_2-structure-dependent (Ziemann and Atkinson, 2012). We do not include these product channels in this study, since they have negligible impacts on the chemical scheme described here. This feature results from two facts: i) we focus on the generic RO_2 and do not explicitly consider the chemistry of products of the different RO_2 loss pathways; ii) the channel producing RO and NO_2 contributes little to NO_2 production (Peng et al., 2018). ~~Despite some small dependencies on the type of RO_2, recommended general rate constants are available for RO_2+HO_2 and RO_2+NO ; Table 1). We use these recommended values for generic RO_2 in this study.~~ However, RO_2 self-/cross-reaction rate constants are highly dependent on the specific RO_2 types and can vary over a very large range (10^{-17}–10^{-10} cm^3 $molecule^{-1}$ s^{-1}). Unsubstituted primary, secondary and tertiary RO_2 self-react at ~10^{-13}, ~10^{-15} and ~10^{-17} cm^3 $molecule^{-1}$ s^{-1}, respectively (Ziemann and Atkinson, 2012). Rate constants of cross-reactions between these RO_2 types also span this range (Orlando and Tyndall, 2012). Substituted RO_2s have higher self-/cross-reaction rate constants (Orlando and Tyndall, 2012). RO_2+RO_2 of highly substituted primary RO_2 can be as high as ~10^{-11} cm^3 $molecule^{-1}$ s^{-1} (Orlando and Tyndall, 2012). Very recently, a few highly oxidized 1,3,5-trimethylbenzene-derived RO_2s were reported to self-/cross-react at ~10^{-10} cm^3 $molecule^{-1}$ s^{-1} (Berndt et al., 2018). In the present work, we make a simplification to adapt to the generic RO_2 treatment by assuming a single self-/cross-reaction rate constant for generic RO_2 in each case. Three levels of RO_2+RO_2 rate constants, i.e. $1x10^{-13}$, $1x10^{-11}$, and $1x10^{-10}$ cm^3 $molecule^{-1}$ s^{-1}, are studied in this paper. The first level is referred to as "medium RO_2+RO_2" as many other RO_2 can have self-/cross-reaction rate constants as low as 10^{-17} cm^3 $molecule^{-1}$ s^{-1}; the second level is defined as "fast RO_2+RO_2"; the last level is called "very fast RO_2+RO_2." No RO_2+RO_2 rate constant lower than the medium level is investigated in the current work, although there are still a large variety of RO_2 whose self-/cross reactions are at lower rate constants, since at the medium level, RO_2+RO_2 is already negligible in all the environments studied in this work, i.e. OFRs, chambers and the atmosphere (see Section 3.1.1). Since there are only a few very specific examples for very fast RO_2+RO_2 reported to date, we will not systematically explore this category but compare very fast RO_2+RO_2 as a sensitivity case with the other two types of RO_2+RO_2 reactions.

Acyl RO_2 is considered as a separate RO_2 type (neither medium nor fast RO_2+RO_2) in this study since its reaction with NO_2 can be a major sink of RO_2 in OFR (Peng and Jimenez, 2017). Thermal decomposition lifetimes of the product of RO_2+NO_2, i.e. acylperoxy nitrates, can be hours at laboratory

temperatures (Orlando and Tyndall, 2012; also taken into account in the current work, see Table 1), while OFR residence times are typically minutes. Besides, acyl RO_2 react with many RO_2 at ~10^{-11} cm^3 $molecule^{-1}$ s^{-1} (Orlando and Tyndall, 2012), similar to that of fast RO_2+RO_2. We thus assume acyl RO_2 self-/cross-reaction rate constant to be also $1x10^{-11}$ cm^3 $molecule^{-1}$ s^{-1} to facilitate the comparison with fast RO_2+RO_2 results.

In OFRs operated at room temperature, acylperoxy nitrates barely decompose, as their thermal decomposition lifetime is typically ~1 h (Orlando and Tyndall, 2012), while OFR residence time is usually a few minutes. In contrast, peroxy nitrates of non-acyl RO_2 do decompose on a timescale of 0.1 s (Orlando and Tyndall, 2012; Table 1). ~~In OFRs operated at room temperature, acylperoxy nitrates barely decompose, while peroxy nitrates of non-acyl RO2 do decompose on a timescale of 0.1 s (Table 1).~~ As a consequence, the production and decomposition of peroxy nitrates of non-acyl RO_2 reach a steady state in OFRs, which can be greatly shifted toward the peroxy nitrate side in cases with very high NO_2 (Peng and Jimenez, 2017; Peng et al., 2018).

RO_2+OH (Fittschen et al., 2014) and RO_2 isomerization (Crounse et al., 2013) have recently been identified as possible significant RO_2 fates in the atmosphere. Reactions of the former type, according to several recent experimental and theoretical studies (Bossolasco et al., 2014; Assaf et al., 2016, 2017b, 2017a; Müller et al., 2016; Yan et al., 2016), have similar rate constants (~$1x10^{-10}$ cm^3 $molecule^{-1}$ s^{-1}) regardless of RO_2 type. Therefore, the reaction rate constant of generic RO_2 with OH is assigned as $1x10^{-10}$ cm^3 $molecule^{-1}$ s^{-1}. RO_2 isomerization reactivity is highly structure-dependent (Crounse et al., 2013; Praske et al., 2018) and rate constant measurements are still scarce, preventing us from assigning a generic RO_2 isomerization rate constant. However, for *generic* RO_2, isomerization is generally *not* a sink but a conversion between two RO_2 (both encompassed by the generic one in this study), as RO_2 isomerization usually generates an oxygenated hydrocarbyl radical, which rapidly recombines with O_2 and forms another RO_2. Therefore, RO_2 isomerization is not explicitly taken into account in the modeling, but is considered in the RO_2 fate analysis.

In summary, 6 pathways are included in the RO_2 fate analysis of this study. The need to explore these 6 pathways for a high number of OFR, chamber, and atmospheric conditions makes presentation of results challenging. For clarity, we present the results in two steps. In the first step, only well-known RO_2 fates (reaction with NO_2, HO_2, NO and RO_2) will be included in the model. In the second step, the results of the first step will be used to guide the modeling and analysis of a more comprehensive set of significant RO_2 fates.

2.3 Model description

The model used in the present work is a standard chemical kinetic box model, implemented in the KinSim 3.4 solver in Igor Pro 7 (WaveMetrics, Lake Oswego, Oregon, USA), and has been described in detail elsewhere (Peng et al., 2015, 2018). Plug flow in the reactor with a residence time of 180 s is assumed, since the effects of non-plug flow are major only in a narrow range of conditions of little experimental interest and the implementation of laminar flow or measured residence time distribution substantially increases computational cost (Peng et al., 2015; Peng and Jimenez, 2017). The reactions

of RO_2 discussed in Section 2.2 are added to the chemical mechanism. A generic slow-reacting VOC (with the same OH rate constant as SO_2) is used as the external OH reactant. Its initial concentration is determined by the initial OHR_{ext} in each model case. Then as this proxy external OH reactant slowly reacts, OHR_{ext} slowly decays. This slow change in OHR_{ext} represents not only the decay of the initial reactant but also the generation and consumption of later-generation products that continue to react with OH.~~This slow rate also represents the generation and consumption of latter-generation products that continue to react with OH.~~ The reason for this approximation has been discussed in detail in previous OFR modeling papers (Peng and Jimenez, 2017; Peng et al., 2018). We exclude NO_y species, which are explicitly modeled, from the calculation of OHR_{ext}; thus OHR_{ext} only includes non-NO_y OHR_{ext} hereafter. As OHR_{ext} is dominated by OHR_{VOC} in most OFR experiments, we use OHR_{ext} to denote OHR_{VOC} in OFRs (while for ambient and chamber cases OHR_{VOC} is still used to exclude the contribution of CO etc.). The outputs of our model (e.g. species concentrations and exposures) were estimated to be accurate to within a factor of 2–3 when compared with field OFR experiments.~~The model was estimated to achieve an accuracy of a factor of 2–3 when compared to field OFR experiments~~; better agreement can generally be obtained for laboratory OFR experiments (Li et al., 2015; Peng et al., 2015).

Another key parameter in the model is the HO_x recycling ratio (β), defined in this study as the number of HO_2 molecule(s) produced per OH molecule destroyed by external OH reactants (Peng et al., 2015). This ratio depends on the products of RO_2 loss pathways. The main product of RO_2+HO_2 is usually ROOH (Table 1), yielding no recycled HO_2, while the main products of RO_2+NO are RO and NO_2, the former of which can often undergo extremely fast H-abstraction by O_2 to form a carbonyl and HO_2. We used the fully chemically explicit (automated chemical mechanism generation based on available knowledge) box-model GECKO-A (Aumont et al., 2005) to simulate OH oxidation of several simple VOCs (e.g. propane and decane) under various OFR conditions with zero-NO. We consistently find that β~0.3.~~From VOC oxidation simulations by the fully explicit model GECKO-A (Aumont et al., 2005), we estimate β~0.3 in zero-NO OFRs.~~ At the other extreme, where RO_2 is solely consumed by RO_2+NO, the product RO yields HO_2 at a branching ratio close to 1, β~1. For intermediate cases, we assume that β may be interpolated as a linear function of $r(RO_2+NO)/[r(RO_2+NO)+r(RO_2+HO_2)]$, where $r(RO_2+NO)$ and $r(RO_2+HO_2)$ are the local reactive fluxes of RO_2+NO and RO_2+HO_2.

In the present work, we model OFR185, OFR254-70, and OFR254-7 (including their -iN_2O variants). We specify the same temperature and atmospheric pressure (295 K and 835 mbar, typical values in Boulder, Colorado, USA) as our previous OFR modeling studies (Li et al., 2015; Peng et al., 2015, 2016, 2018; Peng and Jimenez, 2017). The explored physical condition space follows that of our previous OFR-iN_2O modeling work (Peng et al., 2018). The only differences are that in this study we also include cases without any N_2O injected (OFR185 and OFR254 only) and exclude OHR_{ext}=0 conditions, which produce no RO_2. In detail, the explored physical condition space covers: H_2O of 0.07–2.3% (relative humidity of 2–71% at 295 K); UV photon flux at 185 nm (abbr. F185) of 1.0×10^{11}–1.0×10^{14} photons cm^{-2} s^{-1} [corresponding photon flux at 254 nm (F254) of 4.2×10^{13}–8.5×10^{15} photons cm^{-2} s^{-1}]; OHR_{ext} of 1–1000 s^{-1}; N_2O mixing ratio (abbr. N_2O hereafter) of 0 and 0.02–20%. All model cases are logarithmically evenly

distributed except for N_2O=0 and F254. The latter is calculated based on the F185–F254 relationship for the lamps simulated here (Li et al., 2015).

For the classification of conditions, the same criteria as in the OFR-iN_2O modeling study (Peng et al., 2018) are adopted. In detail, high- and low-NO conditions are classified by $r(RO_2+NO)/r(RO_2+HO_2)$. In the current work, these reactive fluxes are explicitly tracked in the modeling instead of approximated as in previous studies (Peng and Jimenez, 2017; Peng et al., 2018). The terms "good," "risky" and "bad" are used to describe OFR operating conditions in terms of non-tropospheric organic photolysis, and are defined based on the ratios of F185 and F254 exposure ($F185_{exp}$ and $F254_{exp}$, i.e. integrated photon fluxes over residence time) to OH exposure (OH_{exp}), as presented previously (Peng and Jimenez, 2017; Peng et al., 2018). Briefly, under a given condition non-tropospheric photolysis is of different relative importance in the fate of each specific organic species: under good conditions, photolysis at 185 and/or 254 nm is unimportant for almost all VOCs; under bad conditions, non-tropospheric photolysis is problematic for most VOC precursors, since significant photolysis of their oxidation intermediates at 185 and/or 254 nm is almost inevitable; and risky conditions can be problematic for some but not all VOCs. Note that good/risky/bad conditions refer only to non-tropospheric organic photolysis and *not* to whether RO_2 chemistry is atmospherically relevant. Table S1 summarizes our condition classification criteria.

3 Results and discussion

In this section, the results are presented in two parts, i.e. first for the simulations with well-known pathways only, and secondly with all significant pathways, as proposed in Section 2.2. Then based on the results and their comparison with the atmosphere and chamber experiments, we propose guidelines for OFR operation to ensure atmospherically relevant RO_2 chemistry, as well as other chemistries already discussed in the previous studies (Peng et al., 2016, 2018), in OFRs.

3.1 Simulations with well-known pathways (RO_2+HO_2, RO_2+RO_2, RO_2+NO and RO_2+NO_2)

Due to significantly different reactivities of non-acyl and acyl RO_2, the results of these two types of RO_2 are shown separately.

3.1.1 Non-acyl RO_2

In this case non-acyl RO_2 have only three fates, i.e. RO_2+HO_2, RO_2+NO and RO_2+RO_2. The relative importance of these three fates can be shown in a triangle plot (Figure 1). The figure includes data points of OFR185 (including OFR185-iN_2O) and OFR254-70 (including OFR254-70-iN_2O), as well as several typical ambient and chamber studies, including two pristine remote area cases (P_1 and P_2) from the ATom-1 study (Wofsy et al., 2018), two forested area cases (F_1 and F_2) from the BEACHON-RoMBAS and GoAmazon campaigns, respectively (Ortega et al., 2014; Martin et al., 2016, 2017), an urban area case (U) from the CalNex-LA campaign (Ryerson et al., 2013) and five typical chamber experiment cases (C_1–C_5) from the FIXCIT study (Nguyen et al., 2014). These typical cases shown in Fig. 1 bring to light several interesting points: ~~Conditions from the FIXCIT campaign (Nguyen et al., 2014) are used to represent chamber studies as they were designed for specific RO_2 fates within the limitations of current high-quality laboratory chambers (Table 2).~~

- In all ambient and chamber cases, medium and slower RO_2+RO_2 contribute negligibly to the RO_2 fate. This confirms a common impression that self-/cross-reactions of many RO_2 radicals do not significantly affect RO_2 fates.
- However, if RO_2 self-/cross-reacts rapidly, RO_2+RO_2 can be the most important loss pathway among RO_2+RO_2, RO_2+HO_2 and RO_2+NO even in pristine regions with higher VOC (e.g. P_1 in Fig. 1) compared to an average pristine region case (P_2). Note that the P_1 case is still very clean compared to typical forested and urban areas (Table 2).
- Forested areas located in the same region as pollution sources are not as "low-NO" as one may expect (points F_1 and F_2 in Fig. 1). RO_2+NO contributes ~20–50% to RO_2 loss, as NO and HO_2 concentrations are on the same order of magnitude in these cases.
- RO_2+NO dominates over RO_2+RO_2 and RO_2+HO_2 in almost all urban areas. Even in relatively clean urban areas such as Los Angeles during CalNex-LA in 2010 (point U in Fig. 1), average NO is ~1 ppb, still sufficiently high to ensure the dominance of RO_2+NO among the three pathways.
- Various chamber cases in the FIXCIT campaign (low to high OHR_{ext}; low to high NO; points C_x in Fig. 1) are able to represent specific RO_2 fates that appear in different regions in the atmosphere.

On these plots, points for bBad conditions (in terms of non-tropospheric photolysis) are not shown on these plots because of the lack of experimental interest. The triangle plots for OFR254-7 (including OFR254-7-iN_2O) in the same form (Figure S1a,b) show no qualitative differences from the results of OFR254-70, implying that initial O_3 in OFR254 modes has only minor impacts on RO_2 fate. We see this result not only for well-known non-acyl RO_2 fate, but also for the aspects discussed in the following sections. The similarity between OFR254 modes can be explained by the minor effects of a lower O_3 on HO_x at relatively low OHR_{ext} (Peng et al., 2015). Cases at higher OHR_{ext} often have stronger non-tropospheric photolysis (Peng et al., 2016) and hence are more likely to be under bad conditions and are not shown in Figs. 1 and S1a,b. For simplicity, this similarity is not discussed further.

An important feature confirmed in Fig. 1 is that OFR-iN_2O modes effectively realize conditions of experimental interest with variable relative importance of RO_2+NO in RO_2 fate (Lambe et al., 2017; Peng et al., 2018). Tuning initially injected N_2O can achieve this goal (Fig. 2). While it is possible to reduce RO_2+HO_2 in OFR185-iN_2O to negligible compared to RO_2+NO by increasing N_2O, this is not possible in OFR254-70-iN_2O due to fast NO oxidation by the large amounts of O_3 added in the reactor. Nevertheless, OFR254-70-iN_2O can still make RO_2+NO dominate over RO_2+HO_2 in RO_2 fate. OFR and chamber cases span a range of ~0–~100% in relative importance of RO_2+NO in RO_2 fate (Fig. 2), suggesting that both chambers and OFRs are able to ensure the atmospheric relevance of RO_2+NO in RO_2 fate.

Another important feature that can be easily seen in Fig. 1 is that medium rate RO_2+RO_2 (and hence also RO_2+RO_2 slower than 10^{-13} cm^3 $molecule^{-1}$ s^{-1}) are of negligible importance in the fate of RO_2 (Fig. 1a,c) in OFR185 (including OFR185-iN_2O), OFR254-70 (under most conditions, including OFR254-70-iN_2O), chambers and the atmosphere. Thus, a very large subset of RO_2 have only minor or negligible contribution from RO_2+RO_2 to their fate. This is already known for ambient RO_2 fate (Ziemann and

Atkinson, 2012). The reason why this is also true in OFRs is that while OH is much higher than ambient levels, HO_2 and NO (high-NO conditions only) are also higher. One can easily verify that steady-state RO_2 concentrations (see Appendix ~~A~~ B for details) would not deviate from ambient levels by orders of magnitude. The reactive fluxes of RO_2+RO_2 in OFRs are thus not substantially different than in the atmosphere, while RO_2+HO_2 and RO_2+NO (high-NO conditions only) are both faster in OFRs because of higher HO_2 and NO. The combined effect is a *reduced* relative importance of RO_2+RO_2 in RO_2 fate in OFRs compared to the atmosphere. The only exception in OFRs occurs at very high VOC precursor concentrations (OHR_{ext} significantly >100 s^{-1}) in OFR254 (Fig. S2), where OH levels are not substantially suppressed due to large amounts of O_3 (Peng et al., 2015). As a result, RO_2 concentration is remarkably increased by strong production and RO_2+RO_2 relative importance increases roughly quadratically and becomes significant.

The generally lower relative importance of RO_2+RO_2 in OFRs than in the atmosphere is more obvious for the fate of RO_2 with fast RO_2+RO_2 rate constants (Figs. 1b,d and 3). Although OFRs can reasonably reproduce RO_2 fates in typical low- and moderate-OHR_{ext} ambient environments (e.g. typical pristine and forested areas; Figs. 1b,d and 3) and low-OHR_{ext} chambers, OFR185 cannot achieve relative importance of RO_2+RO_2 significantly larger than 50%, such as found in remote environments with higher VOC (e.g. P_1 in Fig. 1) and high-OHR_{ext} chamber experiments (e.g. C_2 and C_5 in Fig. 1; the distribution for C_2 is also shown in Fig. 3). ~~Although OFRs can reasonably reproduce RO_2 fates in low-VOC ambient environments (e.g. typical pristine and forested areas; Figs. 1b,d and 3) and low-OHR_{ext} chambers, OFR185 cannot achieve relative importance of RO_2+RO_2 significantly larger than 50%, corresponding to higher-VOC environments (e.g. P_1 in Fig. 1) and high-OHR_{ext} chamber experiments (e.g. C_2 and C_5 in Fig. 1; the distribution for C_2 is also shown in Fig. 3).~~ In OFR254-70, a relative importance of RO_2+RO_2 as high as ~90% may be attained (Fig. S3). However, this requires very high OHR_{ext}, which leads to medium (and slower) RO_2+RO_2 showing higher-than-ambient relative importance. In reality, fast RO_2+RO_2 all involve substituted RO_2, which almost certainly arise from and coexist with unsubstituted RO_2 (with slower self-/cross reactions). Therefore, very high OHR_{ext} in OFR254 is not really suitable for attaining dominant RO_2+RO_2 conditions. In OFR185, a higher OHR_{ext} generally also results in a higher RO_2+RO_2 relative importance because of higher RO_2 production (Fig. S3). Nevertheless, higher OHR_{ext} is more likely to lead to risky or bad conditions (Fig. 3; Peng et al., 2016). It should be noted that although it is difficult to reliably achieve RO_2+RO_2 with a relative importance larger than 50% in RO_2 fate in OFRs, the distributions of RO_2+RO_2 relative importance in OFRs seems to be within a factor of 2 of those of field/aircraft campaigns (Fig. 3).

In the case of very fast RO_2+RO_2, all features for fast RO_2+RO_2 discussed above are still present (Fig. S1c,d). The only major difference between the results for fast RO_2+RO_2 and very fast RO_2+RO_2 is the significantly higher relative importance of RO_2+RO_2 in RO_2 fate in the latter case, which is expected. In summary, the fast RO_2+RO_2 is not perfectly reproduced in OFRs in terms of relative importance in RO_2 fate, but it is significant when this pathway is also important in the atmosphere.

The HO_x recycling ratio β (see Sect. 2.3) is one of the key factors determining HO_2 in the OFR

model, yet it is not well constrained. Although we make reasonable assumptions for it in the model input (see Section 2.3 for details), a sensitivity study to explore its effects is also performed here. For RO_2 with the fast self-/cross-reaction rate constant, we perform the simulations with the HO_x recycling ratios fixed to a number of values from 0 (radical termination) to 2 (radical proliferation) in lieu of those calculated under the assumptions described in Section 2.3. As expected, the contribution of RO_2+RO_2 to RO_2 fate increases monotonically between β=2 and β=0 (Fig. S4), as the recycling of the competing reactant HO_2 decreases. Nevertheless, the change in the average RO_2+RO_2 relative importance from β=0 to β=2 is generally within a factor of 2. Thus, it still holds that the RO_2+RO_2 relative importance in OFRs is generally lower than in the atmosphere. Only at β~0 may OFR185 theoretically attain a relative importance of RO_2+RO_2 of ~70%, as in the P_1 case (pristine, but relatively high-VOC, Figure S5). Note that β=0 for all VOC oxidation (including oxidation of intermediates) is extremely unlikely. In OFR254, even if RO_2+RO_2 may contribute up to ~100% to RO_2 fate at very high OHR_{ext} at β=0, these conditions still also lead to significant RO_2+RO_2 in the fate of RO_2 that self-/cross-react more slowly, which is not atmospherically relevant.

3.1.2 Acyl RO_2

As described in Section 2.1, the generic acyl RO_2 modeled in this study has the same loss pathways as RO_2 with the fast self-/cross-reaction rate constant, except for RO_2+NO_2, which can be a significant acyl RO_2 loss pathway in OFRs as well as both chambers and atmosphere. When this reaction is included in the simulations of acyl RO_2, it is a minor or negligible loss pathway of RO_2 at low N_2O, while it can be the dominant fate of acyl RO_2 at high N_2O (Fig. 4). In general, the RO_2+NO_2 relative importance increases with initial N_2O. This is always true in OFR254-70-iN_2O between N_2O=0.02% and N_2O=20%, while in OFR185-iN_2O, the average relative contribution of RO_2+NO_2 to RO_2 fate starts to decrease at N_2O~10%, because RO_2+NO regains some importance. This results from the HO_x suppression caused by high NO_y and strong NO production at high N_2O. Strong NO production increases its concentration and suppresses HO_x under these conditions, limiting the conversion of NO to NO_2. Because of the strong OH suppression by high NO_y at N_2O≥10%, these conditions are not desirable (Peng et al., 2018).

The only difference between the simulations of acyl RO_2 and of the fast-self-/cross-reacting non-acyl RO_2 is the quasi-irreversible reaction RO_2+NO_2→RO_2NO_2 at room temperature, whose effects are revealed by a comparison of the triangle plots of the RO_2 fates in each case (Figs. 1b,d and S6). RO_2+NO_2 is clearly dominant in acyl RO_2 fate in OFRs as long as RO_2+NO plays some role (not necessarily under high-NO conditions). In OFR185-iN_2O, the relative importance of RO_2+RO_2 in the sum of the HO_2, NO and RO_2 pathways is reduced (Fig. S6a), compared to that of non-acyl RO_2 with the fast RO_2+RO_2 (Fig. 1b), because RO_2+NO_2 decrease acyl RO_2 concentration. Such a decrease is not significant in OFR254-70-iN_2O (Fig. S6b, compared to Fig. 1d), since for non-acyl RO_2, it is already stored in the form of RO_2NO_2 as RO_2 reservoir. In other words, the high initial O_3 greatly accelerates NO-to-NO_2 oxidation, and shifts the equilibrium RO_2+NO_2↔RO_2NO_2 far to the right even for non-acyl RO_2.

RO_2+NO_2 is an inevitable and dominant sink of most acyl RO_2 in high-NO_x OFRs, though the extent

of this dominance differs substantially between the different OFR operation modes. In OFR254-70-iN_2O, RO_2+NO makes a minor or negligible contribution to acyl RO_2 fate because the required high O_3 very rapidly oxidizes NO to NO_2 and leads to very low NO-to-NO_2 ratios (e.g. ~0.003–0.03; see Fig. S7). In OFR185-iN_2O, the contribution of RO_2+NO can be somewhat significant, with typical NO-to-NO_2 of ~0.03–0.4. (Fig S7). Urban NO-to-NO_2 ratios vary widely, for example (roughly, and excluding significant tails in the frequency distributions), 0.02–1 for Barcelona, 0.007–0.7 for Los Angeles and Pittsburgh (see Fig. S7). Given these variations among different urban areas, RO_2+NO and RO_2+NO_2 for acyl RO_2 in OFR185-iN_2O can be regarded as relevant to urban atmospheres. Exceptions to the relevance of OFR185-iN_2O occur during morning rush hours (e.g. see the high NO-to-NO_2 tail for the Pittsburgh case in Fig. S7), near major NO sources, and/or in urban atmospheres with stronger NO emission intensity (e.g. Beijing, especially in winter; Fig. S7). In these cases, NO-to-NO_2 ratios may significantly exceed 1, and RO_2+NO may be the dominant acyl RO_2 loss pathway. Such high-NO conditions appear difficult to simulate in OFRs with the current range of techniques. ~~RO_2+NO_2 is an inevitable sink of most acyl RO_2 in high-NO_x OFRs. Its contribution to acyl RO_2 fate in OFRs is often higher than in urban atmospheres, where the relative amounts of NO and NO_2 vary overtime. At midday, most NO is usually oxidized to NO_2 in urban atmospheres and RO_2+NO_2 dominates acyl RO_2 fate, as in high-NO_x OFRs. During morning rush hours and/or near major NO sources, NO may be significantly more abundant than NO_2 and RO_2+NO is likely the dominant acyl RO_2 loss pathway, which cannot be simulated in OFRs with the current range of techniques.~~

Acyl RO_2 are not the dominant type among RO_2s under most conditions in OFRs, chambers and the atmosphere, since their formation usually requires multistep (at least 2 steps) oxidation via specific pathways leading to an oxidized end group (i.e. aldehyde and then acylperoxy). However, simulations using the GECKO-A model in urban (Mexico City) and forested (Rocky Mountains) atmospheres (Figure S8) show that acyl RO_2 can still be a major (very roughly 1/3) component of RO_2 at ages of several hours or higher. ~~However, acyl RO_2 can still be a major (very roughly 1/3) source of RO_2 at ages of several hours or higher according to estimations made using the GECKO-A model in urban and forested atmospheres.~~ Therefore, acyl RO_2 chemistry in high-NO OFR can significantly deviate from that in an urban atmosphere with NO dominating NO_x, and can be relevant to an urban atmosphere with NO_2 dominating NO_x. On the other hand, a few theoretical studies suggested that H-abstraction by the acylperoxy radical site from hydroperoxy groups close to the acylperoxy site in multifunctional acyl RO_2 may be extremely fast (Jørgensen et al., 2016; Knap and Jørgensen, 2017). If these theoretical predictions are sufficiently accurate, these acyl RO_2 may exclusively undergo intramolecular H-shift to form non-acyl RO_2 or other radicals and prevent RO_2+NO_2 from occurring even at very high (ppm-level) NO_2. However, this type of RO_2 is structurally specific and may not have strong impacts on the overall acyl RO_2 chemistry.

3.2 Simulations with all significant pathways

Since RO_2 isomerization does not significantly affect the generic RO_2 concentration, the two RO_2 fates that were recently found to be potentially important, i.e. RO_2+OH and RO_2 isomerization, can be

discussed separately.

3.2.1 RO_2+OH

In the troposphere, RO_2+OH is a minor (at low NO) or negligible (at high NO) RO_2 loss pathway (Fittschen et al., 2014; Assaf et al., 2016; Müller et al., 2016), as its rate constant is roughly an-order-of-magnitude higher than that of RO_2+HO_2 (Table 1) while ambient OH concentration is on average 2-orders-of-magnitude lower than that of HO_2 (Mao et al., 2009; Stone et al., 2012; Fig. 5). We will not discuss RO_2+OH in the high-NO cases in detail. Simply put, the relative importance of RO_2+OH is generally negatively correlated with input N_2O in OFR-iN_2O, as NO_x suppresses OH and the relative importance of RO_2+NO increases. Below, we focus on low-NO (actually, for simplicity, zero-NO) conditions.

At N_2O=0, it would be ideal if an HO_2-to-OH ratio identical to the ambient values was realized in OFRs. In OFR185 cases with medium RO_2+RO_2, HO_2-to-OH ratio around 100 occurs at a combination of low H_2O (on the order of 0.1%), low F185 (on the order of 10^{11} photons cm^{-2} s^{-1}), and medium OHR_{ext} (10–100 s^{-1}); and also at medium F185 (~10^{12} photons cm^{-2} s^{-1}) combined with very high OHR_{ext} (~1000 s^{-1}, Fig. ~~S7~~S9). Under both sets of conditions, relatively high external OH reactants suppress OH, whose production is relatively weak, and convert some OH into HO_2 through HO_x recycling in organic oxidation (e.g. via alkoxy radical chemistry). The reason why such an OH-to-HO_2 conversion is needed to attain an ambient-like HO_2-to-OH ratio is that OFR185 is unable to achieve this via the internal (mainly assisted by O_3) interconversion of HO_x. This inability is most evident when F185 (10^{13}–10^{14} photons cm^{-2} s^{-1}) and H_2O (on the order of 1%) are high and OHR_{ext} is low (<~10 s^{-1}; Fig. ~~S7~~S9). Under these conditions, OH production by H_2O photolysis is so strong that the HO_2-to-OH ratio is lowered to ~1, since OH and H (which recombines with O_2 to form HO_2) are produced in equal amounts from H_2O photolysis. As the RO_2+OH rate constant is only roughly 1-order-of-magnitude higher than that for RO_2+HO_2, slightly lower HO_2-to-OH ratios (e.g. ~30) suffice to keep RO_2+OH minor in this case. A combination of UV and H_2O that are not very high and a moderate OHR_{ext} that is able to convert some OH to HO_2 and somewhat elevate the HO_2-to-OH ratio results in minor relative importance RO_2+OH (Figs. ~~S7~~S9 and ~~S8~~S10).

In OFR254-70, it is more difficult to reach an HO_2-to-OH ratio of ~100, which can only be realized at a combination of very low H_2O and F254 (~0.07% and ~5x10^{13} photons cm^{-2} s^{-1}, respectively) and very high OHR_{ext} (~1000 s^{-1}). This is mainly due to high O_3 in OFR254-70, which controls the HO_x interconversion through HO_2+O_3→OH+2O_2 and OH+O_3→HO_2+O_2 and makes both OH and HO_2 more resilient to changes due to OHR_{ext} (Peng et al., 2015). Even without H_2O photolysis at 185 nm as a major HO_2 source, the HO_x interconversion controlled by O_3 in OFR254-70 still brings HO_2-to-OH ratio to ~1 in the case of minimal external perturbation (see the region at the highest H_2O and UV and OHR_{ext}=0 in the OFR254-70 part of Fig. ~~S7~~S9). This ratio cannot be easily elevated in OFR254-70 because of the resilience of OH to suppression for this mode (Peng et al., 2015). Thus, this ratio is relatively low (<30) under most conditions (Fig. ~~S7~~S9), and consequently (and undesirably), RO_2+OH is a major RO_2 fate in OFR254-70. There is an exception at relatively low H_2O and UV with very high OHR_{ext} (Fig. ~~S8~~S10), however these conditions are undesirable in terms of non-tropospheric organic photolysis (Peng et al.,

2016).

Only the results of RO_2 with the medium RO_2+RO_2 are discussed in this subsection. Those of RO_2 with the fast RO_2+RO_2 are not shown as they are not qualitatively different. In OFR185, for the fast-self-/cross-reacting RO_2, RO_2+RO_2 is relatively important at high OHR_{ext} (>~100 s^{-1}; Fig. S3), while RO_2+OH is a major RO_2 fate at low OHR_{ext} (generally on the order of 10 s^{-1} or lower) and relatively high H_2O and UV (Fig. ~~S8~~S10). These two ranges of conditions are relatively far away from each other, and hence there is no condition under which RO_2+RO_2 and RO_2+OH are both major pathways that compete, which simplifies understanding RO_2 fate. However, in OFR254-70, some conditions may lead to both significant RO_2+RO_2 (for the fast-self-/cross-reacting RO_2) and RO_2+OH (e.g. H_2O~0.5%, F254~$1x10^{15}$ photons cm^{-2} s^{-1} and OHR_{ext}~100 s^{-1}). Nevertheless, as long as RO_2+OH plays a major role, these conditions do not bear much experimental interest and thus do not need to be discussed in detail.

3.2.2 RO_2 isomerization

RO_2 isomerization is a first-order reaction. For this type of reactions to occur, RO_2 does not need any other species but only a sufficiently long lifetime against all other reactants combined, as most RO_2 isomerization rate constants are <10 s^{-1}. Radical (OH, HO_2, NO etc.) concentrations in OFRs are much higher than ambient levels and may shorten RO_2 lifetimes compared to those in the troposphere. Possibly reduced RO_2 lifetimes naturally raise concerns over the potentially diminished importance of RO_2 isomerization in OFRs.

In this section we examine generic RO_2 lifetimes against all reactions (calculated without RO_2 isomerization taken into account) in OFR (including OFR-iN_2O) cases (for the medium RO_2+RO_2 case) and compare them with the RO_2 lifetimes in recent major field/aircraft campaigns in relatively clean environments and a field campaign in an urban area (CalNex-LA), as well as a low-NO chamber experiment (Fig. 6). Indeed, RO_2 lifetime in clean ambient cases and in chambers with near-ambient radical levels are generally much longer than those in OFRs. The RO_2 lifetime distribution of the explored good and risky cases in OFR254-70 (including OFR254-70-iN_2O) barely overlaps with the ambient and chamber cases, while in OFR185 (including OFR185-iN_2O), RO_2 lifetime can be as long as ~10 s, which is longer than in urban areas and roughly at the lower end of the range of ambient RO_2 lifetime in clean environments (Fig. 6). The longest RO_2 lifetime in OFR185 occurs at very low F185 (on the order of 10^{11} photons cm^{-2} s^{-1}) and H_2O (~0.1%; Fig. ~~S9~~S11), where HO_x is low. In OFR254-70, for RO_2 to survive for ~10 s, in addition to very low UV and H_2O, high OHR_{ext} is also needed (Fig. ~~S9~~S11). High-OHR_{ext} conditions in OFR254-70 cause OH suppression and a decrease in HO_x concentration, and hence result in relatively long RO_2 lifetimes. However, the strong OH suppression is likely to give bad conditions (high contribution of non-tropospheric photolysis).(Peng et al., 2016) Low-OHR_{ext} conditions do not lead to long RO_2 lifetimes in OFR254-70 even at very low F254 and H_2O, since O_3-assisted HO_x recycling prevents a very low HO_x level even if HO_x primary production is low (Peng et al., 2015)

An RO_2 lifetime (without RO_2 isomerization included) of 10 s leads to a relative importance of isomerization of 50% in the total fate (including all loss pathways) of RO_2 with an isomerization rate constant of 0.1 s^{-1}, which is a typical order of magnitude for isomerization rate constants of

multifunctional RO_2 with hydroxyl and hydroperoxy substituents (Fig. 6; Crounse et al., 2013; D'Ambro et al., 2017; Praske et al., 2018). Although a 50% relative importance of isomerization under some OFR conditions is still lower than those in relatively low-NO ambient environments and low-NO chambers, this relative importance should certainly be deemed major and far from negligible as some have speculated (Crounse et al., 2013). Other monofunctional RO_2 (with peroxy radical site only) and bifunctional RO_2 with peroxy radical site and a carbonyl group isomerize so slowly (~0.001–0.01 s^{-1}) that their isomerizations are minor or negligible loss pathways in the atmosphere, chambers and OFRs with RO_2 lifetimes around 10 s (Fig. 6). Isomerizations of other types of multifunctional RO_2 (e.g. multifunctional acyl RO_2 with hydroxyl and hydroperoxy substituents at favorable positions) are extremely fast (rate constants up to 10^6 s^{-1}; Jørgensen et al., 2016; Knap and Jørgensen, 2017) and always dominate in their fates in the relatively low-NO atmosphere and chambers and OFRs with RO_2 lifetimes around 10 s.

In the discussion about RO_2 isomerization above (as in the RO_2+OH exploration in Section 3.2.1), we only examine low-NO (or zero-NO for simplicity) conditions with medium RO_2+RO_2. In high-NO environments, e.g. polluted urban atmospheres with NO of at least ~10 ppb and high-NO OFRs in the iN_2O modes, RO_2 lifetime is so short that isomerization is no longer a major fate for any but the most rapidly isomerizing multifunctional RO_2 discussed above. NO measured in Los Angeles during the CalNex-LA campaign (Ortega et al., 2016) was only ~1 ppb, which would to allow RO_2 to survive for a few seconds and isomerize (Fig. 6), even in an urban area.

The OFR simulations for the discussions about RO_2 isomerization are the same as those conducted to study RO_2+OH, i.e. the ones with the medium RO_2+RO_2 and RO_2+OH included. For fast RO_2 self-/cross-reaction cases, RO_2 lifetimes may be significantly shorter than for RO_2 with the medium self-/cross-reaction rate constant at high OHR_{ext} (>~100 s^{-1}) in OFR185 (Fig. S3). These high-OHR_{ext} conditions are likely to be risky or bad (of little experimental interest) (Peng et al., 2016) and thus do not need to be discussed further in detail. OFR254-70 (a zero-NO mode) does not generate good or risky (of at least some experimental interest in terms of non-tropospheric organic photolysis) conditions also leading to low-NO-atmosphere-relevant RO_2 lifetimes (Fig. 6). RO_2 with faster self-/cross-reaction rate constants have even shorter lifetimes in OFR254-70 and will not be discussed further.

3.3 Guidelines for OFR operation

In this subsection we discuss OFR operation guidelines for atmospherically relevant RO_2 chemistry, with a focus on OFR185 and OFR254 (zero-NO modes). Since RO_2+HO_2 and RO_2+NO both can vary from negligible to dominant RO_2 fate in OFRs, chambers and the atmosphere (Figs. 1 and 2), these two pathways are not a concern in OFR atmospheric relevance considerations. Neither is the RO_2+RO_2 a major concern. Medium or slower RO_2+RO_2 is minor or negligible in the atmosphere and chambers, as well as in OFRs, as long as high OHR_{ext} is avoided in OFR254 (Fig. S2). Fast RO_2+RO_2 is somewhat less important in OFRs than in the atmosphere (Figs. 1b,d and 3), but is still qualitatively atmospherically relevant, given the uncertainties associated with the HO_x recycling ratios of various reactive systems and the huge variety of RO_2 types (and hence RO_2+RO_2 rate constants).

Accordingly, we focus on the atmospheric relevance of RO_2+OH and RO_2 isomerization, i.e. their relative contributions close to ambient values. Under typical high-NO conditions, RO_2+NO dominates RO_2 fate and RO_2+OH is negligible. High NO also shortens RO_2 lifetime enough to effectively inhibit RO_2 isomerization. Both the dominance of RO_2+NO and the inhibition of RO_2 isomerization also occur in the atmosphere and in chambers, so high-NO OFR operation (typically NO>10 ppb) represents these pathways realistically. Some care is, however, required with the RO_2+OH and RO_2 isomerization pathways at low NO. Since RO_2+HO_2 in OFRs is always a major RO_2 fate at low NO and RO_2+RO_2 are generally not problematic, RO_2+OH and RO_2+HO_2 can be kept atmospherically relevant as long as HO_2-to-OH ratio is close to 100 (the ambient average). In addition, RO_2 lifetime (calculated without RO_2 isomerization taken into account) should be at least around 10 s.

Practically, OH production should be limited to achieve this goal. Too strong OH production at high H_2O and UV can elevate OH and HO_2 concentrations, which shortens RO_2 lifetime, and decreases the HO_2-to-OH ratio to ~1 (see Sect. 3.2.1). OH production is roughly proportional to both H_2O and UV (Peng et al., 2015), so can be limited by reducing either or both. However, H_2O and UV have different effects on non-tropospheric organic photolysis. At a certain OHR_{ext}, OH production rate roughly determines OH concentration in OFRs. Reducing UV decreases both OH and UV roughly proportionally (Peng et al., 2015), and hence changes in $F185_{exp}/OH_{exp}$ and $F254_{exp}/OH_{exp}$ are small (Peng et al., 2016); i.e. non-tropospheric organic photolysis does not become significantly worse if UV is reduced. By contrast, if H_2O is reduced without also decreasing UV, $F185_{exp}/OH_{exp}$ and $F254_{exp}/OH_{exp}$ both increase, signifying stronger relative importance of non-tropospheric photolysis. Therefore, reducing UV is strongly preferred as an OH production limitation method, and is effective in making both RO_2+OH and RO_2 isomerization more atmospherically relevant.

To further explore the effects of UV reduction on the RO_2+OH (Fig. 5) and RO_2 isomerization (Fig. 6) pathways, we divide our OFR case distributions into higher-UV and lower-UV classes, with the boundary being the mid-level (in logarithmic scale) UV in the explored range. The distributions for lower-UV conditions (solid lines in Figs. 5 and 6) are clearly closer to the ambient cases (i.e. HO_2-to-OH ratio closer to 100, smaller RO_2+OH relative importance and longer RO_2 lifetime).

Since OFR254 is unable to achieve both conditions with at least some experimental interest (i.e. with sufficiently low non-tropospheric photolysis) and atmospherically relevant RO_2 lifetime, we now discuss preferable conditions for OFR185 only. As F185 close to or lower than 10^{12} photons cm^{-2} s^{-1} is needed for RO_2 lifetime to be around 10 s or longer (Fig. ~~S9~~S11), the OH concentration under preferable conditions for atmospherically relevant RO_2 chemistry (~10^9 molecules cm^{-3} or lower) is much lower than the maximum that OFR185 can physically reach (~10^{10}–10^{11} molecules cm^{-3}). Furthermore, lower OH production leads to higher susceptibility to OH suppression by external OH reactants (Peng et al., 2015), which can create non-tropospheric photolysis problems (Peng et al., 2016). We thus recommend as high H_2O as possible to maintain practically high OH while allowing lower UV to limit the importance of non-tropospheric organic photolysis.

The performance of various OFR185 conditions at high H_2O (2.3%) is illustrated in Fig. 7 as a

function of F185 and OHR_{ext}. The three criteria for the performance, i.e. RO_2 lifetime (calculated without RO_2 isomerization considered), relative importance of RO_2+OH and log($F254_{exp}/OH_{exp}$) (a measure of 254 nm non-tropospheric photolysis, which is usually worse than that at 185 nm; Peng et al., 2016) are shown. At F185 of ~10^{11}–10^{12} photons cm^{-2} s^{-1} and OHR_{ext} around or lower than 10 s^{-1}, all three criteria are satisfied. Since UV (and hence OH production) is relatively low, a low OHR_{ext} (~10 s^{-1}) is required to avoid heavy OH suppression and keep conditions good (green area in the bottom panel of Fig. 7). Nevertheless, risky conditions [log($F254_{exp}/OH_{exp}$)<7; light red area in the bottom panel of Fig. 7] may also bear some experimental conditions depending on the type of VOC precursors (specifically on their reactivity toward OH and their photolability at 185 and 254 nm, and the same quantities for their oxidation intermediates; Peng et al., 2016; Peng and Jimenez, 2017). Thus, higher OHR_{ext} (up to ~100 s^{-1}) may also be considered in OFR experiments with some precursors (e.g. alkanes). In practice, the preferred conditions may require F185 even lower than that our lowest simulated lamp setting (Li et al., 2015). Such a low F185 may be realized e.g. by partially blocking 185 nm photons using non-transparent lamp sleeves with evenly placed holes that allow some 185 nm transmission.

Under these preferred conditions, OH concentration in OFR185 is ~10^9 molecules cm^{-3}, equivalent to a photochemical age of ~1 eq. d for a typical residence time of 180 s. This is much shorter than ages corresponding to the maximal oxidation capacity of OFRs (usually eq. weeks or months; Peng et al., 2015) but it is similar to the ages of the maximal organic aerosol formation in OFRs processing ambient air (Tkacik et al., 2014; Ortega et al., 2016; Palm et al., 2016). We show the maximal SOA formation case in the OFR185 experiments in the BEACHON-RoMBAS campaign in the Rocky Mountains (Palm et al., 2016) as an example (Figs. 5 and 6). During the campaign, relative humidity was high (>60% in most of the period), OHR_{ext} was estimated to be relatively low (~15 s^{-1}) in this forested area, and UV in the OFR was limited in the case of the maximal SOA formation age (~0.7 eq. d). All these physical conditions were favorable for atmospherically relevant RO_2 fate (Figs. 5 and 6). RO_2+OH was minor in this case and the relative importance of RO_2 isomerization in RO_2 fate in the OFR was within a factor of ~2 of that in the atmosphere for all RO_2 (regardless of isomerization rate constant) during the BEACHON-RoMBAS campaign (Fig. 6). The effect of UV on the relative importance of RO_2 isomerization for this example is also illustrated in Fig. 6. In the sensitivity case with a lower age, a lower UV results in a larger contribution of isomerization to RO_2 fate, while the relative importance of RO_2 isomerization is lower in a sensitivity case with an age 3 times of that of the maximal SOA formation. In an extreme sensitivity case with the highest UV in the range of this study (with an age of 4 eq. mo), RO_2 isomerization becomes minor or negligible for all RO_2 except extremely rapidly isomerizing ones.

The discussions above indicate that the atmospheric relevance of gas-phase RO_2 chemistry in OFRs deteriorates as the photochemical age over the whole residence time (180 s) increases. To reach longer ages, longer residence times (with UV being still low) can be adopted. However, OFR residence times > 10 min tend to be limited by the increasing importance of wall losses (Palm et al., 2016). As a result, longer residence times can only increase photochemical age in OFRs up to about a week. This implies that in OFR cases with ages much higher than that of maximal SOA formation (corresponding to the

heterogeneous oxidation stage of SOA), the atmospheric relevance of gas-phase RO_2 chemistry in the SOA formation stage (before the age of maximal SOA formation) often cannot be ensured. However, under those conditions typically new SOA formation is not observed, and the dominant process affecting OA is heterogeneous oxidation of the pre-existing OA (Palm et al., 2016). If the heterogeneous oxidation of the newly formed SOA is of interest, a two-stage solution may be required. Lower UV can be used in the SOA formation stage to keep the atmospheric relevance of the gas-phase chemistry, while high UV can be used in the heterogeneous aging stage to reach a high equivalent age. The latter approach is viable since heterogeneous oxidation of SOA by OH is slow and partide-phase chemistry is not strongly affected by gas-phase species except OH, when OH is very high (Richards-Henderson et al., 2015, 2016; Hu et al., 2016). This two-stage solution may be realized through a cascade-OFR system or UV sources at different intensities within an OFR (e.g. spliced lamps).

Praske et al. (2018) measured RO_2 isomerization rate constants at 296 and 318 K and observed an increase in the rate constants by a factor of ~5 on average. A 15 K temperature increase in OFRs would lead to RO_2 isomerization being accelerated by a factor of ~3, while other major gas-phase radical reactions have weak or no temperature-dependence (e.g. ~7%, ~5%, ~6% and ~19% slow-downs for isoprene+OH, toluene+OH, typical RO_2+NO and RO_2+HO_2, respectively; (Atkinson and Arey, 2003; Ziemann and Atkinson, 2012). As a consequence, the relative importance of RO_2 isomerization in RO_2 fate in OFRs can be elevated and closer to atmospheric values (Fig. 6). Nevertheless, a 15 K increase in temperature may also result in some OA evaporation (Huffman et al., 2009; Nault et al., 2018). Besides, reduction of acylperoxy nitrate formation in OFRs, which may be useful to mimic some urban environments where NO plays a larger role in acyl RO_2 fate (see Section 3.1.2), is unlikely to be achieved by increasing OFR temperature. The O-N bond energy of acylperoxy nitrates is ~28 kcal/mol (Orlando and Tyndall, 2012), which can be taken as an approximate reaction energy of their decomposition. Then a 20 K temperature increase results in the equilibrium constant of acyl RO_2+NO_2↔acyl RO_2NO_2 shifted toward RO_2+NO_2 by a factor of ~20. However, this shift is still too small relative to the equilibrium constant itself. It can be obtained by a simple calculation that for the generic acyl RO_2 in this study in an OFR at 318 K (20 K higher than room temperature) with NO_2 of 10^{12} molecules cm^{-3} (a relatively low level in typical OFR-iN_2O experiments; (Peng et al., 2018), ~0.1% of the total amount of acyl RO_2 + acyl RO_2NO_2 will be present in the form of acyl RO_2. Even if acylperoxy nitrate decomposition is x20 faster than at room temperature and the formed acyl RO_2 can irreversibly react with NO and decrease acylperoxy nitrate concentration, this effect is small: typically up to ~20% decrease in acylperoxy nitrate and usually negligible changes in NO and NO_2. The minor effect is due to i) acylperoxy concentration that is still very low, ii) NO concentration that is much lower than NO_2, and iii) acylperoxy nitrate decomposition lifetime that is still on the order of minutes.

As discussed above, high H_2O, low UV and low OHR_{ext} are recommended for keeping the atmospheric relevance of RO_2 chemistry in OFRs. These three requirements are also part of the requirements for attaining good high-NO conditions in OFR185-iNO (the OFR185 mode with initial NO injection; Peng and Jimenez, 2017). In addition to these three, an initial NO of several tens of ppb is also

needed to obtain a good high-NO condition in OFR185-iNO. Under these conditions, RO_2+NO dominates over RO_2+HO_2, and hence RO_2+OH; UV is low, the photochemical age is typically ~1 eq. d, and RO_2 lifetime can be a few seconds. Therefore, these conditions are a good fit for studying the environments in relatively clean urban areas, such as Los Angeles during CalNex-LA (Ortega et al., 2016), where NO is high enough that the dominant bimolecular fate of RO_2 is RO_2+NO but low enough to maintain RO_2 lifetimes that allow most common RO_2 isomerizations.

As RO_2 fate in OFRs is a highly complex problem and it can be tricky to find suitable physical conditions to simultaneously achieve experimental goals and keep the atmospheric relevance of the chemistry in OFRs, we provide here an OFR RO_2 Fate Estimator (in Supplement) to qualitatively aid experimental planning. The OFR RO_2 Fate Estimator couples the OFR Exposure Estimator (Peng et al., 2016, 2018) to a General RO_2 Fate Estimator (also in Supplement, see Fig. ~~S10~~ S12 for a screenshot of its layout). The OFR Exposure Estimator updated in this study also contains estimation equations for the HO_2-to-OH ratio in OFR185 (in OFR254, RO_2 fate is always atmospherically irrelevant at low NO, while at high NO, RO_2+NO dominates and a detailed RO_2 fate analysis is no longer needed). In the General RO_2 Fate Estimator, all RO_2 reactant concentrations and all RO_2 loss pathway rate constants can be specified. Thus the General RO_2 Fate Estimator can also be applied to the atmosphere and chamber experiments, in addition to OFRs. When applied to OFRs, the General RO_2 Fate Estimator is provided by the OFR RO_2 Fate Estimator with quantities estimated in the OFR Exposure Estimator (e.g. OH and NO). RO_2 concentration and fate are calculated according to Appendix ~~A~~ B in the RO_2 Fate Estimators.

4 Conclusions

We investigated RO_2 chemistry in OFRs with an emphasis on its atmospheric relevance. All potentially major loss pathways of RO_2, i.e. reactions of RO_2 with HO_2, NO and OH, that of acyl RO_2 with NO_2, self-/cross-reactions of RO_2 and RO_2 isomerization, were studied and their relative importance in RO_2 fate were compared to those in the atmosphere and chamber experiments. OFRs were shown to be able to tune the relative importance of RO_2+HO_2 vs. RO_2+NO by injecting different amounts of N_2O. For many RO_2 (including all unsubstituted non-acyl RO_2 and substituted secondary and tertiary RO_2), their self-reactions and the cross-reaction between them are minor or negligible in the atmosphere and chambers. This is also the case in OFR185 (including OFR185-iN_2O) and OFR254-iN_2O, however those RO_2 self-/cross-reactions can be important at high precursor concentrations (OHR_{ext}>100 s^{-1}) in OFR254. For substituted primary RO_2 and acyl RO_2, their self-/cross-reactions (including the ones with RO_2 whose self-reaction rate constants are slower) can play an important role in RO_2 fate in the atmosphere and chambers, and may also be major RO_2 loss pathways in OFRs, although they are somewhat less important in OFRs than in the atmosphere. Acylperoxy nitrates are the dominant sink of acyl RO_2 at high NO_x in OFRs (particularly in OFR254-iN_2O where RO_2+NO is negligible for acylperoxy loss), while only a minor reservoir of acyl RO_2 in the atmosphere under most conditions except in urban atmospheres, where RO_2+NO and RO_2+NO_2 ~~acylperoxy nitrate formation~~ can both be the dominant acylperoxy loss pathway ~~when most NO is oxidized to NO_2~~ depending on conditions. In chambers, most acyl RO_2 can be stored in the form of acylperoxy nitrates if NO_2 is very high (hundreds of ppb to ppm level).

Formatted: Subscript

Besides the above-mentioned well-known pathways, RO_2+OH and RO_2 isomerization may also play an important role in RO_2 fate and sometimes result in atmospherically irrelevant RO_2 chemistry in OFRs. Here we summarize the main findings about all the pathways and the related guidelines for OFR operation:

- Under typical high-NO conditions, RO_2+NO dominates RO_2 fate and RO_2 lifetime is too short to allow most RO_2 isomerizations, regardless of whether in the atmosphere, chambers or OFRs, thus raising no concern about the atmospheric relevance of the OFR RO_2 chemistry.
- Under low-NO conditions, OFR254 cannot yield any physical conditions leading to sufficiently long RO_2 lifetime for its isomerization because of the high radical levels and their resilience to external perturbations in OFR254.
- In OFR185 with strong OH production (and hence high OH), RO_2+OH and RO_2 isomerization may strongly deviate from that in the atmosphere [becoming important and negligible, respectively, for relatively rapidly isomerizing RO_2 (rate constants on the order of 0.1 s^{-1})].
- To attain both atmospherically relevant VOC and RO_2 chemistries, OFR185 requires high H_2O, low UV and low OHR_{ext}. These conditions ensure minor or negligible RO_2+OH and a relative importance of RO_2 isomerization in RO_2 fate in OFRs within a factor of ~2 of that in the atmosphere.
- Under conditions allowing both VOC and RO_2 chemistries to be atmospherically relevant, the maximal photochemical age that can be reached is limited to a few eq. days. This age roughly covers the period required for maximum SOA formation in ambient air.
- To most realistically study much higher ages for SOA functionalization/fragmentation by heterogeneous oxidation, a sequence of low-UV SOA formation followed by a high UV condition (in the same reactor or in cascade reactors) may be needed.
- High H_2O, low UV and low OHR_{ext} in the OFR185-iNO mode can achieve conditions relevant to clean urban atmosphere, i.e. high-NO but not sufficiently high to inhibit common RO_2 isomerization. ~~Under typical high-NO conditions, RO_2+NO dominates RO_2 fate and RO_2 lifetime is too short to allow most RO_2 isomerizations, regardless of whether in the atmosphere, chambers or OFRs, thus raising no concern over the atmospheric relevance of the OFR RO_2 chemistry. However, under low-NO conditions, OFR254 cannot yield any physical conditions leading to sufficiently long RO_2 lifetime for its isomerization because of the high radical levels and their resilience to external perturbations in OFR254. In OFR185 with strong OH production (and hence high OH), RO_2+OH and RO_2 isomerization may strongly deviate from the atmosphere (becoming important and negligible, respectively, for relatively rapidly isomerizing RO_2). To attain both atmospherically relevant VOC and RO_2 chemistries, OFR185 requires high H_2O, low UV and low OHR_{ext}, which conditions ensure minor or negligible RO_2+OH and a relative importance of RO_2 isomerization in RO_2 fate in OFRs within x~2 of that in the atmosphere but limit the maximal photochemical age that can be reached to a few eq. days. This age roughly covers SOA formation in ambient air up to its maximum. To reach a much~~

~~higher age for studying SOA functionalization/fragmentation by heterogeneous oxidation, a sequence of low-UV SOA formation followed by a high-UV condition (in the same reactor or in cascade reactors) would be needed. High H_2O, low UV and low OHR_{ext} in the OFR185-iNO mode can achieve conditions relevant to clean urban atmosphere, i.e. high NO but not sufficiently high to inhibit common RO_2 isomerization.~~

Finally, RO_2 chemistry is not only highly complex but also plays a central and instrumental role in atmospheric chemistry, in particular VOC oxidation and SOA formation. For all experiments conducted with atmospheric chemistry simulation apparatus (chambers, flow reactors etc.), an atmospherically relevant RO_2 chemistry is crucial to meaningful experimental results. However, most literature studies did not publish experimental data that are sufficient for estimating RO_2 fate. The FIXCIT chamber experiment campaign is one of the few exceptions where comprehensive data were reported (Nguyen et al., 2014) and used for the RO_2 fate analysis in the present work. We recommend measuring and/or estimating and reporting OH, HO_2, NO, NO_2 and OHR_{VOC} (or initial precursor composition at least) whenever possible, for all future atmospheric laboratory and field experiments for organic oxidation to facilitate the analysis of RO_2 fate and the evaluation of its atmospheric relevance.

Appendix A: Glossary of the acronyms (except field campaign names) used in the paper

OFR	oxidation flow reactor
VOC	volatile organic compound
SOA	secondary organic aerosol
H_2O	water vapor mixing ratio
OHR_{ext}	external OH reactivity (due to CO, SO_2, VOCs etc.)
PAM	Potential Aerosol Mass, a specific type of OFR
OFR185	oxidation flow reactor using both 185 and 254 nm light
OFR254	oxidation flow reactor using 254 nm light only
OFR254-X	OFR254 with X ppm O_3 initially injected
OFR-iN_2O	OFR with N_2O initially injected
OFR185-iN_2O	OFR185 with N_2O initially injected
OFR254-iN_2O	OFR254 with N_2O initially injected
OFR254-X-iN_2O	OFR254-X with N_2O initially injected
OHR_{VOC}	OH reactivity due to VOCs

F185, F254 etc.	UV photon flux at 185 nm, 254 nm etc.
N_2O	N_2O mixing ratio
OH_{exp}, $F185_{exp}$ etc.	exposure (integral over time) to OH, F185 etc.

Appendix AB: Steady-state approximation for generic RO_2

The production rate of a generic RO_2 is almost identical to the VOC consumption rate, since the second step of the conversion chain VOC→R→RO_2 is extremely fast. Therefore, the generic RO_2 production rate, *P*, can be expressed as follows:

$$P = \sum_i k_i c_i \cdot \mathrm{OH} = \mathrm{OHR}_{\mathrm{VOC}} \cdot \mathrm{OH} \quad \text{(A1)}$$

where OH is OH concentration and c_i and k_i are respectively the concentration and the reaction rate constant with OH of the i^{th} VOC. OHR_{VOC} is the total OHR due to VOC and equal to $\Sigma_i k_i c_i$ by definition.

For the generic RO_2 loss rate, the reactions of RO_2 with HO_2, NO, RO_2, NO_2 (for acyl RO_2 only) and OH are considered. Isomerization generally does not lead to a total RO_2 concentration decrease and is thus not included in its loss rate. Then the RO_2 loss rate is

$$L = k_{\mathrm{HO_2}}\mathrm{RO_2} \cdot \mathrm{HO_2} + k_{\mathrm{NO}}\mathrm{RO_2} \cdot \mathrm{NO} + 2k_{\mathrm{RO_2}}\mathrm{RO_2} \cdot \mathrm{RO_2} + k_{\mathrm{NO_2}}\mathrm{RO_2} \cdot \mathrm{NO_2} + k_{\mathrm{OH}}\mathrm{RO_2} \cdot \mathrm{OH} \quad \text{(A2)}$$

where RO_2, HO_2, NO, NO_2 and OH are the concentrations of corresponding species and k_A (A = RO_2, HO_2, NO, NO_2 and OH) is the reaction rate constant of RO_2 with A. For non-acyl RO_2, the term $k_{\mathrm{NO_2}}\mathrm{RO_2} \cdot \mathrm{NO_2}$ is not included; for cases with well-known pathways only (RO_2+HO_2, RO_2+RO_2, RO_2+NO and RO_2+NO_2; see Section 3.1), the term $k_{\mathrm{OH}}\mathrm{RO_2} \cdot \mathrm{OH}$ is excluded. $k_{\mathrm{RO_2}}$ needs to be given a value (which may be the main levels of RO_2 self-/cross-reaction rate constants in this study, 1×10^{-13} and 1×10^{-11} cm^3 $molecule^{-1}$ s^{-1}, or other values depending on the RO_2 type).

At the steady state, *P* and *L* are equal. For an ambient/chamber setting, OH, HO_2, NO, NO_2 and OHR_{VOC} are often measured or known. In this case, simultaneously considering Eqs. A1 and A2 yields a quadratic equation of RO_2 concentration (the only unknown). Then generic RO_2 concentration can be easily obtained by solving this equation:

$$\mathrm{RO_2} = \left(-K + \sqrt{K^2 + 8k_{\mathrm{RO_2}} \cdot \mathrm{OHR}_{\mathrm{VOC}} \cdot \mathrm{OH}}\right) / \left(4k_{\mathrm{RO_2}}\right) \quad \text{(A3)}$$

where $K = k_{\mathrm{HO_2}}\mathrm{HO_2} + k_{\mathrm{NO}}\mathrm{NO} + k_{\mathrm{NO_2}}\mathrm{NO_2} + k_{\mathrm{OH}}\mathrm{OH}$.

Conflicts of interest

There are no conflicts to declare.

Acknowledgements

This work was partially supported by grants EPA STAR 83587701-0, NSF AGS-1740610, NSF AGS-1822664, NASA NNX15AT96G, and DOE(BER/ASR) DE-SC0016559. We thank the following individuals for providing data from atmospheric field studies: Tran Nguyen and Jordan Krechmer (FIXCIT), William Brune (SOAS and ATom), Pedro Campuzano-Jost (ATom), Daun Jeong and Saewung Kim (GoAmazon), Weiwei Hu (Beijing). We are also grateful to John Crounse, Joel Thornton, Paul Ziemann, Dwayne Heard, Paul Wennberg, Andrew Lambe and William Brune for useful discussions and Donna Sueper for her

assistance in the development of the RO_2 Fate Estimator. NCAR is sponsored by the National Science Foundation. EPA has not reviewed this manuscript and thus no endorsement should be inferred.

References

Assaf, E., Song, B., Tomas, A., Schoemaecker, C. and Fittschen, C.: Rate Constant of the Reaction between CH3O2 Radicals and OH Radicals Revisited, J. Phys. Chem. A, 120(45), 8923–8932, doi:10.1021/acs.jpca.6b07704, 2016.

Assaf, E., Tanaka, S., Kajii, Y., Schoemaecker, C. and Fittschen, C.: Rate constants of the reaction of C2–C4 peroxy radicals with OH radicals, Chem. Phys. Lett., 684, 245–249, doi:10.1016/j.cplett.2017.06.062, 2017a.

Assaf, E., Sheps, L., Whalley, L., Heard, D., Tomas, A., Schoemaecker, C. and Fittschen, C.: The Reaction between CH3O2 and OH Radicals: Product Yields and Atmospheric Implications, Environ. Sci. Technol., 51(4), 2170–2177, doi:10.1021/acs.est.6b06265, 2017b.

Assaf, E., Schoemaecker, C., Vereecken, L. and Fittschen, C.: Experimental and theoretical investigation of the reaction of RO2 radicals with OH radicals: Dependence of the HO2 yield on the size of the alkyl group, Int. J. Chem. Kinet., 50(9), 670–680, doi:10.1002/kin.21191, 2018.

Atkinson, R. and Arey, J.: Atmospheric degradation of volatile organic compounds., Chem. Rev., 103(12), 4605–38, doi:10.1021/cr0206420, 2003.

Aumont, B., Szopa, S. and Madronich, S.: Modelling the evolution of organic carbon during its gas-phase tropospheric oxidation: development of an explicit model based on a self generating approach, Atmos. Chem. Phys., 5(9), 2497–2517, doi:10.5194/acp-5-2497-2005, 2005.

Berndt, T., Scholz, W., Mentler, B., Fischer, L., Herrmann, H., Kulmala, M. and Hansel, A.: Accretion Product Formation from Self- and Cross-Reactions of RO2 Radicals in the Atmosphere, Angew. Chemie Int. Ed., 57(14), 3820–3824, doi:10.1002/anie.201710989, 2018.

Bossolasco, A., Faragó, E. P., Schoemaecker, C. and Fittschen, C.: Rate constant of the reaction between CH3O2 and OH radicals, Chem. Phys. Lett., 593(2014), 7–13, doi:10.1016/j.cplett.2013.12.052, 2014.

Burkholder, J. B., Sander, S. P., Abbatt, J., Barker, J. R., Huie, R. E., Kolb, C. E., Kurylo, M. J., Orkin, V. L., Wilmouth, D. M. and Wine, P. H.: Chemical Kinetics and Photochemical Data for Use in Atmospheric Studies: Evaluation Number 18, Pasadena, CA, USA. [online] Available from: http://jpldataeval.jpl.nasa.gov/, 2015.

Carter, W. P. L., Cocker, D. R., Fitz, D. R., Malkina, I. L., Bumiller, K., Sauer, C. G., Pisano, J. T., Bufalino, C. and Song, C.: A new environmental chamber for evaluation of gas-phase chemical mechanisms and secondary aerosol formation, Atmos. Environ., 39(40), 7768–7788, doi:10.1016/j.atmosenv.2005.08.040, 2005.

Cocker, D. R., Flagan, R. C. and Seinfeld, J. H.: State-of-the-Art Chamber Facility for Studying Atmospheric Aerosol Chemistry, Environ. Sci. Technol., 35(12), 2594–2601, doi:10.1021/es0019169, 2001.

Crounse, J. D., Nielsen, L. B., Jørgensen, S., Kjaergaard, H. G. and Wennberg, P. O.: Autoxidation of organic compounds in the atmosphere, J. Phys. Chem. Lett., 4, 3513–3520, doi:10.1021/jz401920 7, 2013.

D'Ambro, E. L., Møller, K. H., Lopez-Hilfiker, F. D., Schobesberger, S., Liu, J., Shilling, J. E., Lee, B. H., Kjaergaard, H. G. and Thornton, J. A.: Isomerization of Second-Generation Isoprene Peroxy Radicals: Epoxide Formation and Implications for Secondary Organic Aerosol Yields, Environ. Sci. Technol., 51(9), 4978–4987, doi:10.1021/acs.est.7b00460, 2017.

Fittschen, C., Whalley, L. K. and Heard, D. E.: The reaction of CH3O2 radicals with OH radicals: a neglected sink for CH3O2 in the remote atmosphere., Environ. Sci. Technol., 48(14), 7700–1, doi:10.1021/es502481q, 2014.

Fry, J. L., Draper, D. C., Zarzana, K. J., Campuzano-Jost, P., Day, D. A., Jimenez, J. L., Brown, S. S., Cohen, R. C., Kaser, L., Hansel, A., Cappellin, L., Karl, T., Hodzic Roux, A., Turnipseed, A., Cantrell, C., Lefer, B. L. and Grossberg, N.: Observations of gas- and aerosol-phase organic nitrates at BEACHON-RoMBAS 2011, Atmos. Chem. Phys., 13(17), 8585–8605, doi:10.5194/acp-13-8585-2013, 2013.

Hu, W., Palm, B. B., Day, D. A., Campuzano-Jost, P., Krechmer, J. E., Peng, Z., de Sá, S. S., Martin, S. T., Alexander, M. L., Baumann, K., Hacker, L., Kiendler-Scharr, A., Koss, A. R., de Gouw, J. A., Goldstein, A. H., Seco, R., Sjostedt, S. J., Park, J.-H., Guenther, A. B., Kim, S., Canonaco, F., Prévôt, A. S. H., Brune, W.

H. and Jimenez, J. L.: Volatility and lifetime against OH heterogeneous reaction of ambient isoprene-epoxydiols-derived secondary organic aerosol (IEPOX-SOA), Atmos. Chem. Phys., 16(18), 11563–11580, doi:10.5194/acp-16-11563-2016, 2016.

Huffman, J. A., Docherty, K. S., Aiken, A. C., Cubison, M. J., Ulbrich, I. M., DeCarlo, P. F., Sueper, D., Jayne, J. T., Worsnop, D. R., Ziemann, P. J. and Jimenez, J. L.: Chemically-resolved aerosol volatility measurements from two megacity field studies, Atmos. Chem. Phys., 9(1), 7161–7182, doi:doi:10.5194/acp-9-7161-2009, 2009.

Jørgensen, S., Knap, H. C., Ørkjær, R. V, Jensen, A. M., Kjeldsen, M. L. H., Wennberg, P. O. and Kjaergaard, H. G.: Rapid Hydrogen Shift Scrambling in Hydroperoxy-Substituted Organic Peroxy Radicals, J. Phys. Chem. A, 120(2), 266–275, doi:10.1021/acs.jpca.5b06768, 2016.

Kalafut-Pettibone, A. J., Klems, J. P., Burgess, D. R. and McGivern, W. S.: Alkylperoxy radical photochemistry in organic aerosol formation processes., J. Phys. Chem. A, 117(51), 14141–50, doi:10.1021/jp4094996, 2013.

Kang, E., Root, M. J., Toohey, D. W. and Brune, W. H.: Introducing the concept of Potential Aerosol Mass (PAM), Atmos. Chem. Phys., 7(22), 5727–5744, doi:10.5194/acp-7-5727-2007, 2007.

Kang, E., Toohey, D. W. and Brune, W. H.: Dependence of SOA oxidation on organic aerosol mass concentration and OH exposure: experimental PAM chamber studies, Atmos. Chem. Phys., 11(4), 1837–1852, doi:10.5194/acp-11-1837-2011, 2011.

Karjalainen, P., Timonen, H., Saukko, E., Kuuluvainen, H., Saarikoski, S., Aakko-Saksa, P., Murtonen, T., Bloss, M., Dal Maso, M., Simonen, P., Ahlberg, E., Svenningsson, B., Brune, W. H., Hillamo, R., Keskinen, J. and Rönkkö, T.: Time-resolved characterization of primary particle emissions and secondary particle formation from a modern gasoline passenger car, Atmos. Chem. Phys., 16(13), 8559–8570, doi:10.5194/acp-16-8559-2016, 2016.

Klems, J. P., Lippa, K. a and McGivern, W. S.: Quantitative Evidence for Organic Peroxy Radical Photochemistry at 254 nm, J. Phys. Chem. A, 119(2), 344–351, doi:10.1021/jp509165x, 2015.

Knap, H. C. and Jørgensen, S.: Rapid Hydrogen Shift Reactions in Acyl Peroxy Radicals, J. Phys. Chem. A, 121(7), 1470–1479, doi:10.1021/acs.jpca.6b12787, 2017.

Krechmer, J. E., Pagonis, D., Ziemann, P. J. and Jimenez, J. L.: Quantification of Gas-Wall Partitioning in Teflon Environmental Chambers Using Rapid Bursts of Low-Volatility Oxidized Species Generated in Situ, Environ. Sci. Technol., 50(11), 5757–5765, doi:10.1021/acs.est.6b00606, 2016.

Lambe, A., Massoli, P., Zhang, X., Canagaratna, M., Nowak, J., Daube, C., Yan, C., Nie, W., Onasch, T., Jayne, J., Kolb, C., Davidovits, P., Worsnop, D. and Brune, W.: Controlled nitric oxide production via O(¹D) + N₂ reactions for use in oxidation flow reactor studies, Atmos. Meas. Tech., 10(6), 2283–2298, doi:10.5194/amt-10-2283-2017, 2017.

Lambe, A. T. and Jimenez, J. L.: PAM Wiki: User Groups, [online] Available from: https://sites.google.com/site/pamwiki/user-groups (Accessed 2 July 2018), 2018.

Lambe, A. T., Ahern, A. T., Williams, L. R., Slowik, J. G., Wong, J. P. S., Abbatt, J. P. D., Brune, W. H., Ng, N. L., Wright, J. P., Croasdale, D. R., Worsnop, D. R., Davidovits, P. and Onasch, T. B.: Characterization of aerosol photooxidation flow reactors: heterogeneous oxidation, secondary organic aerosol formation and cloud condensation nuclei activity measurements, Atmos. Meas. Tech., 4(3), 445–461, doi:10.5194/amt-4-445-2011, 2011.

Lambe, A. T., Cappa, C. D., Massoli, P., Onasch, T. B., Forestieri, S. D., Martin, A. T., Cummings, M. J., Croasdale, D. R., Brune, W. H., Worsnop, D. R. and Davidovits, P.: Relationship between Oxidation Level and Optical Properties of Secondary Organic Aerosol, Environ. Sci. Technol., 47(12), 6349–6357, doi:10.1021/es401043j, 2013.

Lambe, A. T., Chhabra, P. S., Onasch, T. B., Brune, W. H., Hunter, J. F., Kroll, J. H., Cummings, M. J., Brogan, J. F., Parmar, Y., Worsnop, D. R., Kolb, C. E. and Davidovits, P.: Effect of oxidant concentration, exposure time, and seed particles on secondary organic aerosol chemical composition and yield, Atmos. Chem. Phys., 15(6), 3063–3075, doi:10.5194/acp-15-3063-2015, 2015.

Levy II, H.: Normal atmosphere: large radical and formaldehyde concentrations predicted., Science,

173(3992), 141–143, doi:10.1126/science.173.3992.141, 1971.

Li, R., Palm, B. B., Ortega, A. M., Hu, W., Peng, Z., Day, D. A., Knote, C., Brune, W. H., de Gouw, J. and Jimenez, J. L.: Modeling the radical chemistry in an Oxidation Flow Reactor (OFR): radical formation and recycling, sensitivities, and OH exposure estimation equation, J. Phys. Chem. A, 119(19), 4418–4432, doi:10.1021/jp509534k, 2015.

Lim, C. Y., Browne, E. C., Sugrue, R. A. and Kroll, J. H.: Rapid heterogeneous oxidation of organic coatings on submicron aerosols, Geophys. Res. Lett., 44(6), 2949–2957, doi:10.1002/2017GL072585, 2017.

Link, M. F., Friedman, B., Fulgham, R., Brophy, P., Galang, A., Jathar, S. H., Veres, P., Roberts, J. M. and Farmer, D. K.: Photochemical processing of diesel fuel emissions as a large secondary source of isocyanic acid (HNCO), Geophys. Res. Lett., 43(8), 4033–4041, doi:10.1002/2016GL068207, 2016.

Mao, J., Ren, X., Brune, W. H., Olson, J. R., Crawford, J. H., Fried, a., Huey, L. G., Cohen, R. C., Heikes, B., Singh, H. B., Blake, D. R., Sachse, G. W., Diskin, G. S., Hall, S. R. and Shetter, R. E.: Airborne measurement of OH reactivity during INTEX-B, Atmos. Chem. Phys., 9(1), 163–173, doi:10.5194/acp-9-163-2009, 2009.

Martin, S. T., Artaxo, P., Machado, L. A. T., Manzi, A. O., Souza, R. A. F., Schumacher, C., Wang, J., Andreae, M. O., Barbosa, H. M. J., Fan, J., Fisch, G., Goldstein, A. H., Guenther, A., Jimenez, J. L., Pöschl, U., Silva Dias, M. A., Smith, J. N. and Wendisch, M.: Introduction: Observations and Modeling of the Green Ocean Amazon (GoAmazon2014/5), Atmos. Chem. Phys., 16(8), 4785–4797, doi:10.5194/acp-16-4785-2016, 2016.

Martin, S. T., Artaxo, P., Machado, L., Manzi, A. O., Souza, R. A. F., Schumacher, C., Wang, J., Biscaro, T., Brito, J., Calheiros, A., Jardine, K., Medeiros, A., Portela, B., De Sá, S. S., Adachi, K., Aiken, A. C., Albrecht, R., Alexander, L., Andreae, M. O., Barbosa, H. M. J., Buseck, P., Chand, D., Comstmstmstock, J. M., Day, D. A., Dubey, M., Fan, J., Fastst, J., Fisch, G., Fortner, E., Giangrande, S., Gillles, M., Goldststein, A. H., Guenther, A., Hubbbbe, J., Jensen, M., Jimenez, J. L., Keutstsch, F. N., Kim, S., Kuang, C., Laskskin, A., McKinney, K., Mei, F., Millller, M., Nascimento, R., Pauliquevis, T., Pekour, M., Peres, J., Petäjä, T., Pöhlklker, C., Pöschl, U., Rizzo, L., Schmid, B., Shilllling, J. E., Silva Dias, M. A., Smith, J. N., Tomlmlinson, J. M., Tóta, J. and Wendisch, M.: The green ocean amazon experiment (GOAMAZON2014/5) observes pollution affecting gases, aerosols, clouds, and rainfall over the rain forest, Bull. Am. Meteorol. Soc., 98(5), 981–997, doi:10.1175/BAMS-D-15-00221.1, 2017.

Matsunaga, A. and Ziemann, P. J.: Gas-Wall Partitioning of Organic Compounds in a Teflon Film Chamber and Potential Effects on Reaction Product and Aerosol Yield Measurements, Aerosol Sci. Technol., 44(10), 881–892, doi:10.1080/02786826.2010.501044, 2010.

Müller, J.-F., Liu, Z., Nguyen, V. S., Stavrakou, T., Harvey, J. N. and Peeters, J.: The reaction of methyl peroxy and hydroxyl radicals as a major source of atmospheric methanol, Nat. Commun., 7(May), 13213, doi:10.1038/ncomms13213, 2016.

Nault, B. A., Campuzano-Jost, P., Day, D. A., Schroder, J. C., Anderson, B., Beyersdorf, A. J., Blake, D. R., Brune, W. H., Choi, Y., Corr, C. A., de Gouw, J. A., Dibb, J., DiGangi, J. P., Diskin, G. S., Fried, A., Huey, L. G., Kim, M. J., Knote, C. J., Lamb, K. D., Lee, T., Park, T., Pusede, S. E., Scheuer, E., Thornhill, K. L., Woo, J.-H. and Jimenez, J. L.: Secondary Organic Aerosol Production from Local Emissions Dominates the Organic Aerosol Budget over Seoul, South Korea, during KORUS-AQ, Atmos. Chem. Phys. Discuss., 1–69, doi:10.5194/acp-2018-838, 2018.

Nel, A.: Air Pollution-Related Illness: Effects of Particles, Science (80-.)., 308(5723), 804–806, doi:10.1126/science.1108752, 2005.

Nguyen, T. B., Crounse, J. D., Schwantes, R. H., Teng, A. P., Bates, K. H., Zhang, X., St. Clair, J. M., Brune, W. H., Tyndall, G. S., Keutsch, F. N., Seinfeld, J. H. and Wennberg, P. O.: Overview of the Focused Isoprene eXperiment at the California Institute of Technology (FIXCIT): mechanistic chamber studies on the oxidation of biogenic compounds, Atmos. Chem. Phys., 14(24), 13531–13549, doi:10.5194/acp-14-13531-2014, 2014.

Orlando, J. J. and Tyndall, G. S.: Laboratory studies of organic peroxy radical chemistry: an overview with emphasis on recent issues of atmospheric significance, Chem. Soc. Rev., 41(19), 6294, doi:10.1039/c2cs35166h, 2012.

Ortega, A. M., Day, D. A., Cubison, M. J., Brune, W. H., Bon, D., de Gouw, J. A. and Jimenez, J. L.:

970 Secondary organic aerosol formation and primary organic aerosol oxidation from biomass-burning
971 smoke in a flow reactor during FLAME-3, Atmos. Chem. Phys., 13(22), 11551–11571, doi:10.5194/acp-
972 13-11551-2013, 2013.

973 Ortega, A. M., Hayes, P. L., Peng, Z., Palm, B. B., Hu, W., Day, D. A., Li, R., Cubison, M. J., Brune, W. H.,
974 Graus, M., Warneke, C., Gilman, J. B., Kuster, W. C., de Gouw, J., Gutiérrez-Montes, C. and Jimenez, J. L.:
975 Real-time measurements of secondary organic aerosol formation and aging from ambient air in an
976 oxidation flow reactor in the Los Angeles area, Atmos. Chem. Phys., 16(11), 7411–7433,
977 doi:10.5194/acp-16-7411-2016, 2016.

978 Ortega, J., Turnipseed, A., Guenther, A. B., Karl, T. G., Day, D. A., Gochis, D., Huffman, J. A., Prenni, A. J.,
979 Levin, E. J. T., Kreidenweis, S. M., DeMott, P. J., Tobo, Y., Patton, E. G., Hodzic, A., Cui, Y. Y., Harley, P. C.,
980 Hornbrook, R. S., Apel, E. C., Monson, R. K., Eller, A. S. D., Greenberg, J. P., Barth, M. C., Campuzano-Jost,
981 P., Palm, B. B. B., Jimenez, J. L., Aiken, A. C., Dubey, M. K., Geron, C., Offenberg, J., Ryan, M. G., Fornwalt,
982 P. J., Pryor, S. C., Keutsch, F. N., Digangi, J. P., Chan, A. W. H., Goldstein, A. H., Wolfe, G. M., Kim, S., Kaser,
983 L., Schnitzhofer, R., Hansel, A., Cantrell, C. A., Mauldin, R. L. and Smith, J. N.: Overview of the Manitou
984 experimental forest observatory: Site description and selected science results from 2008 to 2013, Atmos.
985 Chem. Phys., 14(12), 6345–6367, doi:10.5194/acp-14-6345-2014, 2014.

986 Palm, B. B., Campuzano-Jost, P., Ortega, A. M., Day, D. A., Kaser, L., Jud, W., Karl, T., Hansel, A., Hunter, J.
987 F., Cross, E. S., Kroll, J. H., Peng, Z., Brune, W. H. and Jimenez, J. L.: In situ secondary organic aerosol
988 formation from ambient pine forest air using an oxidation flow reactor, Atmos. Chem. Phys., 16(5),
989 2943–2970, doi:10.5194/acp-16-2943-2016, 2016.

990 Palm, B. B., Campuzano-Jost, P., Day, D. A., Ortega, A. M., Fry, J. L., Brown, S. S., Zarzana, K. J., Dube, W.,
991 Wagner, N. L., Draper, D. C., Kaser, L., Jud, W., Karl, T., Hansel, A., Gutiérrez-Montes, C. and Jimenez, J.
992 L.: Secondary organic aerosol formation from in situ OH, O3, and NO3 oxidation of ambient forest air in
993 an oxidation flow reactor, Atmos. Chem. Phys., 17(8), 5331–5354, doi:10.5194/acp-17-5331-2017, 2017.

994 Peng, Z. and Jimenez, J. L.: Modeling of the chemistry in oxidation flow reactors with high initial NO,
995 Atmos. Chem. Phys., 17(19), 11991–12010, doi:10.5194/acp-17-11991-2017, 2017.

996 Peng, Z., Day, D. A., Stark, H., Li, R., Lee-Taylor, J., Palm, B. B., Brune, W. H. and Jimenez, J. L.: HOx radical
997 chemistry in oxidation flow reactors with low-pressure mercury lamps systematically examined by
998 modeling, Atmos. Meas. Tech., 8(11), 4863–4890, doi:10.5194/amt-8-4863-2015, 2015.

999 Peng, Z., Day, D. A., Ortega, A. M., Palm, B. B., Hu, W., Stark, H., Li, R., Tsigaridis, K., Brune, W. H. and
1000 Jimenez, J. L.: Non-OH chemistry in oxidation flow reactors for the study of atmospheric chemistry
1001 systematically examined by modeling, Atmos. Chem. Phys., 16(7), 4283–4305, doi:10.5194/acp-16-
1002 4283-2016, 2016.

1003 Peng, Z., Palm, B. B., Day, D. A., Talukdar, R. K., Hu, W., Lambe, A. T., Brune, W. H. and Jimenez, J. L.:
1004 Model Evaluation of New Techniques for Maintaining High-NO Conditions in Oxidation Flow Reactors
1005 for the Study of OH-Initiated Atmospheric Chemistry, ACS Earth Sp. Chem., 2(2), 72–86,
1006 doi:10.1021/acsearthspacechem.7b00070, 2018.

1007 Platt, S. M., El Haddad, I., Zardini, a. a., Clairotte, M., Astorga, C., Wolf, R., Slowik, J. G., Temime-Roussel,
1008 B., Marchand, N., Ježek, I., Drinovec, L., Močnik, G., Möhler, O., Richter, R., Barmet, P., Bianchi, F.,
1009 Baltensperger, U. and Prévôt, a. S. H.: Secondary organic aerosol formation from gasoline vehicle
1010 emissions in a new mobile environmental reaction chamber, Atmos. Chem. Phys., 13(18), 9141–9158,
1011 doi:10.5194/acp-13-9141-2013, 2013.

1012 Praske, E., Otkjær, R. V., Crounse, J. D., Hethcox, J. C., Stoltz, B. M., Kjaergaard, H. G. and Wennberg, P.
1013 O.: Atmospheric autoxidation is increasingly important in urban and suburban North America, Proc. Natl.
1014 Acad. Sci., 115(1), 64–69, doi:10.1073/pnas.1715540115, 2018.

1015 Presto, A. A., Huff Hartz, K. E. and Donahue, N. M.: Secondary Organic Aerosol Production from Terpene
1016 Ozonolysis. 1. Effect of UV Radiation, Environ. Sci. Technol., 39(18), 7036–7045,
1017 doi:10.1021/es050174m, 2005.

1018 Richards-Henderson, N. K., Goldstein, A. H. and Wilson, K. R.: Large Enhancement in the Heterogeneous
1019 Oxidation Rate of Organic Aerosols by Hydroxyl Radicals in the Presence of Nitric Oxide, J. Phys. Chem.
1020 Lett., 6, 4451–4455, doi:10.1021/acs.jpclett.5b02121, 2015.

1021 Richards-Henderson, N. K., Goldstein, A. H. and Wilson, K. R.: Sulfur Dioxide Accelerates the
1022 Heterogeneous Oxidation Rate of Organic Aerosol by Hydroxyl Radicals, Environ. Sci. Technol., 50(7),
1023 3554–3561, doi:10.1021/acs.est.5b05369, 2016.

1024 Ryerson, T. B., Andrews, A. E., Angevine, W. M., Bates, T. S., Brock, C. A., Cairns, B., Cohen, R. C., Cooper,
1025 O. R., De Gouw, J. A., Fehsenfeld, F. C., Ferrare, R. A., Fischer, M. L., Flagan, R. C., Goldstein, A. H., Hair,
1026 J. W., Hardesty, R. M., Hostetler, C. A., Jimenez, J. L., Langford, A. O., McCauley, E., McKeen, S. A., Molina,
1027 L. T., Nenes, A., Oltmans, S. J., Parrish, D. D., Pederson, J. R., Pierce, R. B., Prather, K., Quinn, P. K., Seinfeld,
1028 J. H., Senff, C. J., Sorooshian, A., Stutz, J., Surratt, J. D., Trainer, M., Volkamer, R., Williams, E. J. and Wofsy,
1029 S. C.: The 2010 California Research at the Nexus of Air Quality and Climate Change (CalNex) field study,
1030 J. Geophys. Res. Atmos., 118(11), 5830–5866, doi:10.1002/jgrd.50331, 2013.

1031 Stocker, T. F., Qin, D., Plattner, G.-K., Tignor, M., Allen, S. K., Boschung, J., Nauels, A., Xia, Y., Bex, V. and
1032 Midgley, P. M.: Climate Change 2013 - The Physical Science Basis, edited by Intergovernmental Panel on
1033 Climate Change, Cambridge University Press, Cambridge., 2014.

1034 Stone, D., Whalley, L. K. and Heard, D. E.: Tropospheric OH and HO2 radicals: field measurements and
1035 model comparisons, Chem. Soc. Rev., 41(19), 6348, doi:10.1039/c2cs35140d, 2012.

1036 Tkacik, D. S., Lambe, A. T., Jathar, S., Li, X., Presto, A. A., Zhao, Y., Blake, D., Meinardi, S., Jayne, J. T.,
1037 Croteau, P. L. and Robinson, A. L.: Secondary Organic Aerosol Formation from in-Use Motor Vehicle
1038 Emissions Using a Potential Aerosol Mass Reactor, Environ. Sci. Technol., 48(19), 11235–11242,
1039 doi:10.1021/es502239v, 2014.

1040 Wang, J., Doussin, J. F., Perrier, S., Perraudin, E., Katrib, Y., Pangui, E. and Picquet-Varrault, B.: Design of
1041 a new multi-phase experimental simulation chamber for atmospheric photosmog, aerosol and cloud
1042 chemistry research, Atmos. Meas. Tech., 4(11), 2465–2494, doi:10.5194/amt-4-2465-2011, 2011.

1043 Wofsy, S. C., Apel, E., Blake, D. R., Brock, C. A., Brune, W. H., Bui, T. P., Daube, B. C., Dibb, J. E., Diskin, G.
1044 S., Elkiins, J. W., Froyd, K., Hall, S. R., Hanisco, T. F., Huey, L. G., Jimenez, J. L., McKain, K., Montzka, S. A.,
1045 Ryerson, T. B., Schwarz, J. P., Stephens, B. B., Weinzierl, B. and Wennberg, P.: ATom: Merged Atmospheric
1046 Chemistry, Trace Gases, and Aerosols, Oak Ridge, Tennessee, USA., 2018.

1047 Yan, C., Kocevska, S. and Krasnoperov, L. N.: Kinetics of the Reaction of CH3O2 Radicals with OH Studied
1048 over the 292–526 K Temperature Range, J. Phys. Chem. A, 120(31), 6111–6121,
1049 doi:10.1021/acs.jpca.6b04213, 2016.

1050 Zhang, X., Cappa, C. D., Jathar, S. H., McVay, R. C., Ensberg, J. J., Kleeman, M. J. and Seinfeld, J. H.:
1051 Influence of vapor wall loss in laboratory chambers on yields of secondary organic aerosol., Proc. Natl.
1052 Acad. Sci. U. S. A., 111(16), 5802–7, doi:10.1073/pnas.1404727111, 2014.

1053 Ziemann, P. J. and Atkinson, R.: Kinetics, products, and mechanisms of secondary organic aerosol
1054 formation, Chem. Soc. Rev., 41(19), 6582, doi:10.1039/c2cs35122f, 2012.

1055

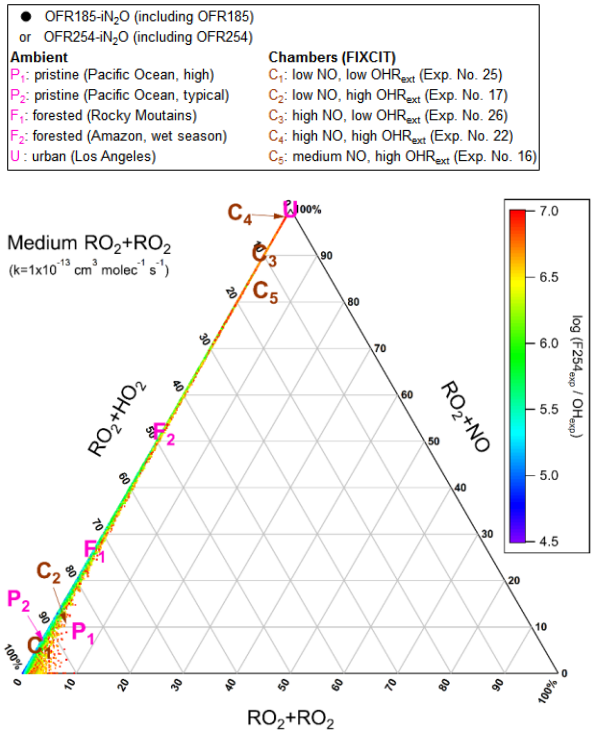

1056

1057

1058 **(a) OFR185**

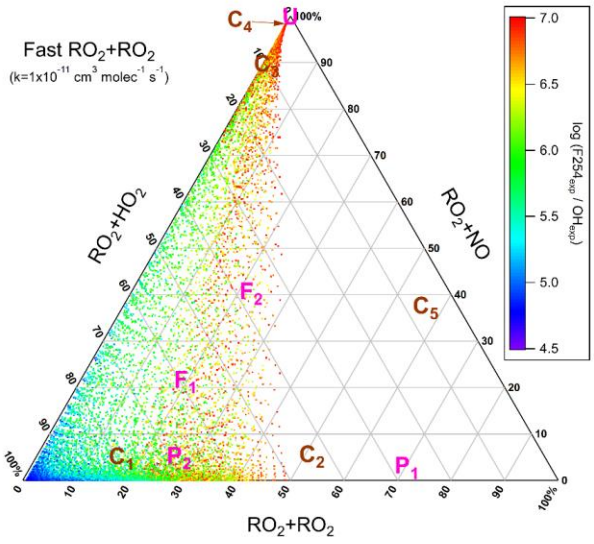

1059

1060 **(b) OFR185**

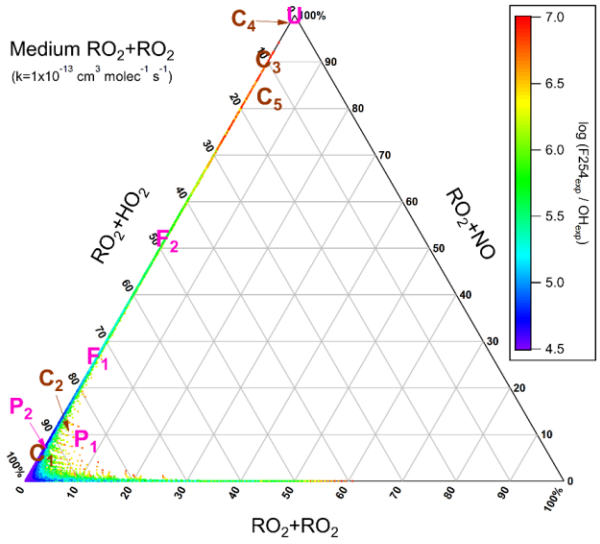

1061

1062 **(c) OFR254-70**

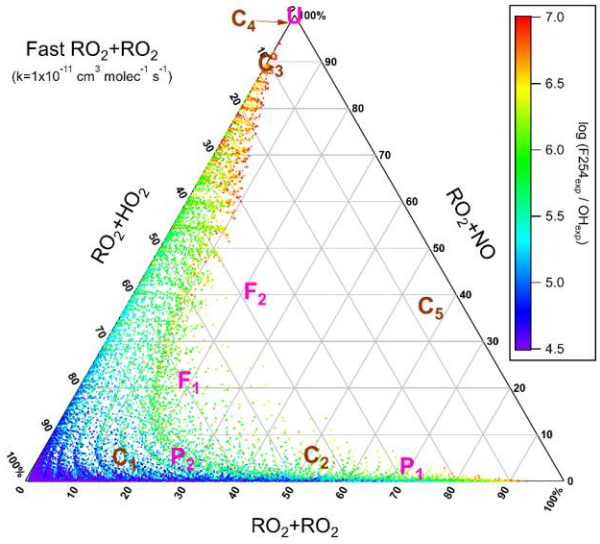

1063

1064 **(d) OFR254-70**

1065 **Figure 1.** Triangle plots of RO_2 fate by RO_2+HO_2, RO_2+RO_2 and RO_2+NO (without RO_2+OH and RO_2
1066 isomerization considered in the model) for RO_2 with the medium self/cross reaction rate constant ($1x10^{-13}$
1067 cm^{-3} $molecule^{-1}$ s^{-1}) in (a) OFR185 (including OFR185-iN_2O) and (c) OFR254-70 (induding OFR254-70-
1068 iN_2O) and for RO2 with the fast self/cross reaction rate constant ($1x10^{-11}$ cm^{-3} $molecule^{-1}$ s^{-1}) in (b)
1069 OFR185 (including OFR185-iN_2O) and (d) OFR254-70 (including OFR254-70-iN_2O). Inclined tick values on
1070 an axis indicate the grid lines that should be followed (in parallel to the inclination) to read the

corresponding values on this axis. The OFR data points are colored by the logarithm of the exposure ratio between 254 nm photon flux and OH, a measure of badness of OFR conditions in terms of 254 nm organic photolysis. Several typical ambient and chamber cases (see Table 2 for details of these cases) are also shown for comparison.

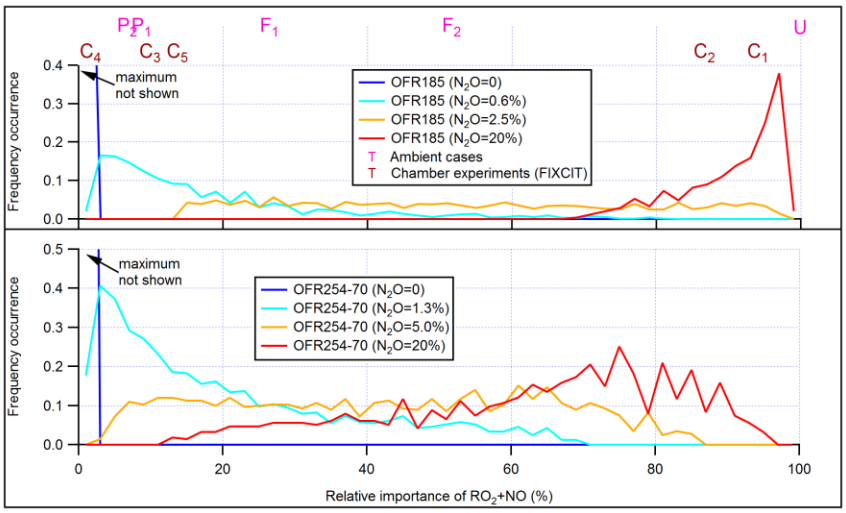

Figure 2. Frequency distributions of the relative importance of RO_2+NO in the fate of RO_2 (with medium self/cross reaction rate constant and without RO_2+OH and RO_2 isomerization considered) for OFR185 (including OFR185-iN_2O) and OFR254-70 (including OFR254-70-iN_2O). Distributions for several different N_2O levels are shown. Only good and risky conditions (in terms of non-tropospheric organic photolysis) are included in the distributions. Also shown is the relative importance of RO_2+NO for several typical ambient and chamber cases (see Table 2 for details of these cases).

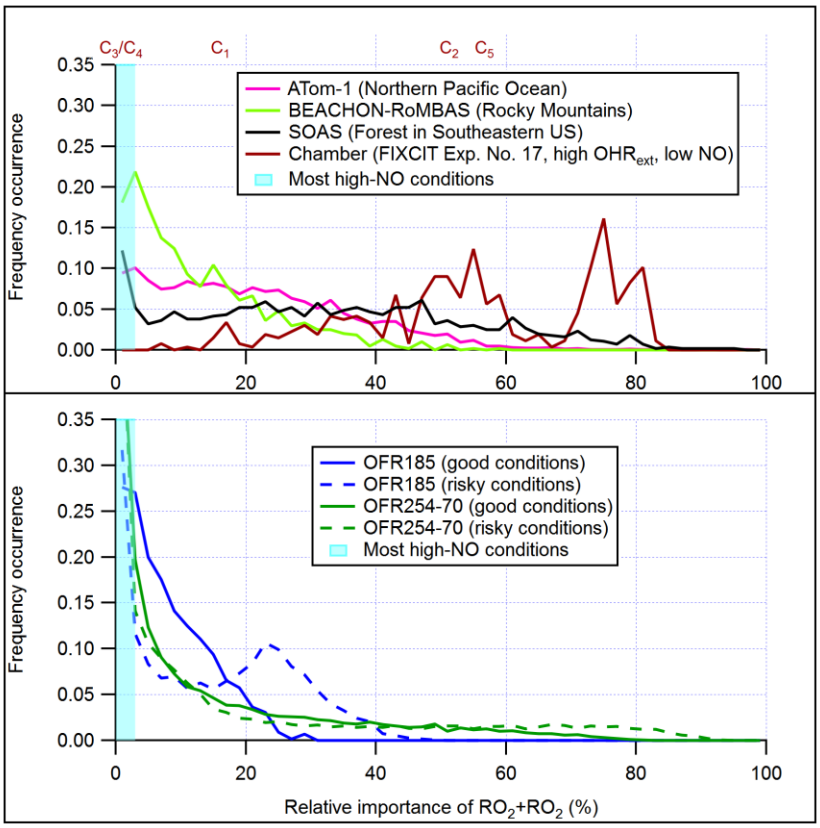

Figure 3. Frequency distributions of the relative importance of RO_2+RO_2 in the fate of RO_2 (with fast self/cross reaction rate constant and without RO_2+OH and RO_2 isomerization considered) for OFR185 (including OFR185-iN_2O), OFR254-70 (including OFR254-70-iN_2O) and a chamber experiment and in the atmosphere (a couple of different environments). The OFR distributions for good and risky conditions (in terms of 254 nm organic photolysis, see Table S1 for the definitions of these conditions) are shown separately. Also shown is the relative importance of RO_2+RO_2 for several typical chamber cases (see Table 2 for details of these cases). The range of the RO_2+RO_2 relative importance for most high-NO conditions is highlighted in cyan.

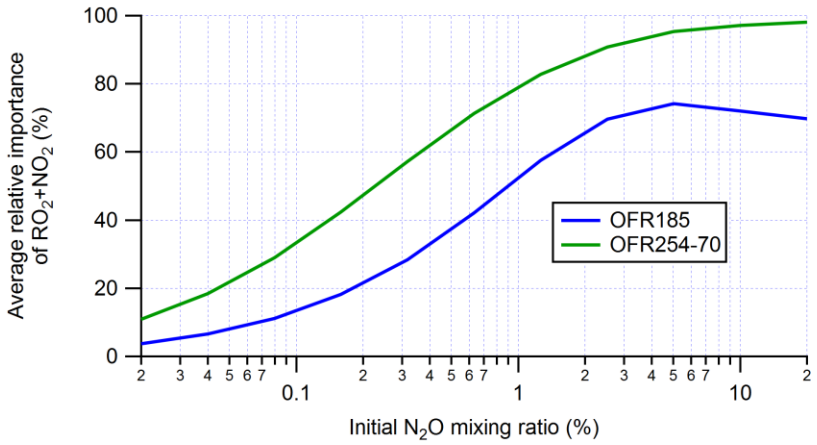

Figure 4. Average relative importance of RO_2+NO_2 in acyl RO_2 fate (RO_2+OH and RO_2 isomerization not considered) in OFR185 (including OFR185-iN_2O) and OFR254-70 (including OFR254-70-iN_2O). The averages are calculated based on good and risky conditions (in terms of non-tropospheric organic photolysis) only.

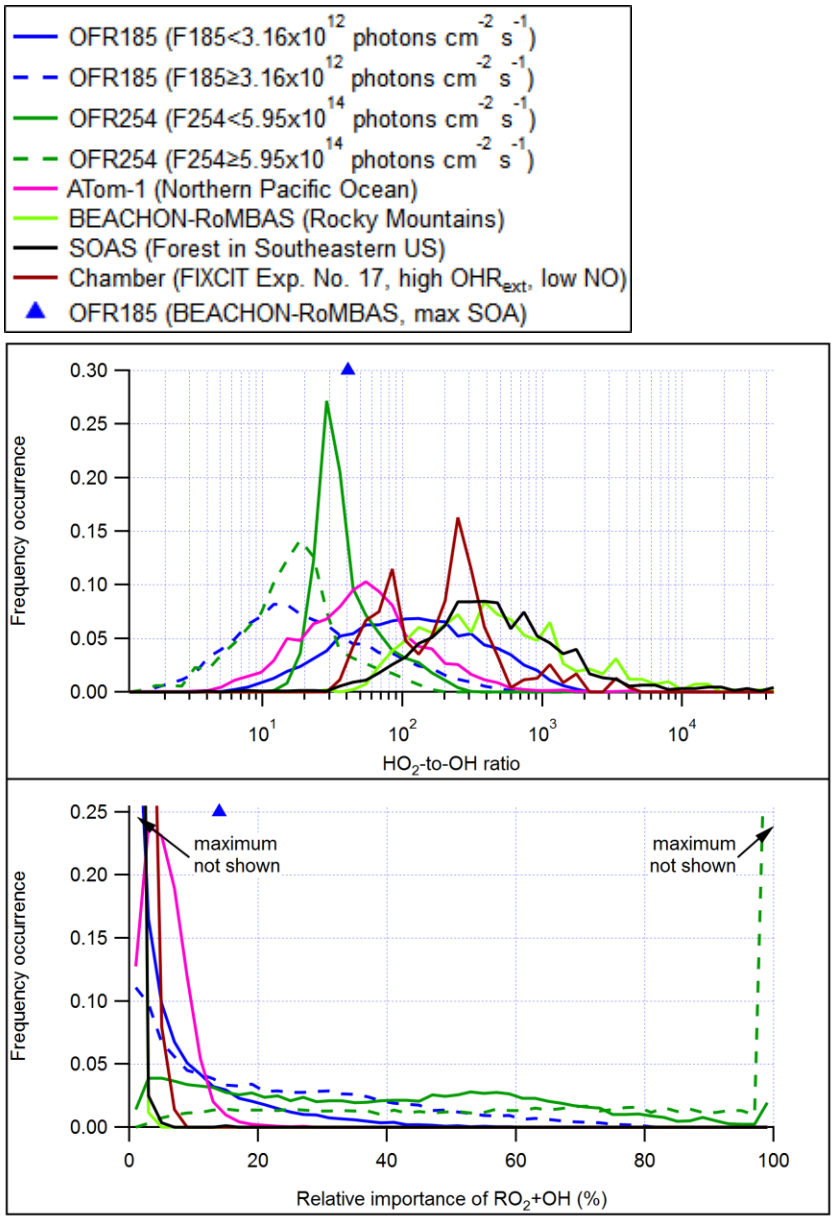

Figure 5. Frequency distributions of (top) the HO_2-to-OH ratio and (bottom) the relative importance of RO_2+OH in the fate of RO_2 (with medium self/cross reaction rate constant) for OFR185 (including OFR185-iN_2O), OFR254-70 (including OFR254-70-iN_2O) and a chamber experiment and in the atmosphere (a couple of different environments). The OFR distributions for lower (F185<3.16x10^{12} photons cm^{-2} s^{-1}; F254<5.95x10^{14} photons cm^{-2} s^{-1}) and higher UV (F185≥3.16x10^{12} photons cm^{-2} s^{-1}; F254≥5.95x10^{14} photons cm^{-2} s^{-1}) are shown separately. Only good and risky conditions (in terms of non-tropospheric organic photolysis) are included in the distributions for OFRs. Also shown are the HO_2-to-OH and the relative importance of RO_2+OH for OFR experiments with ambient air input in field studies.

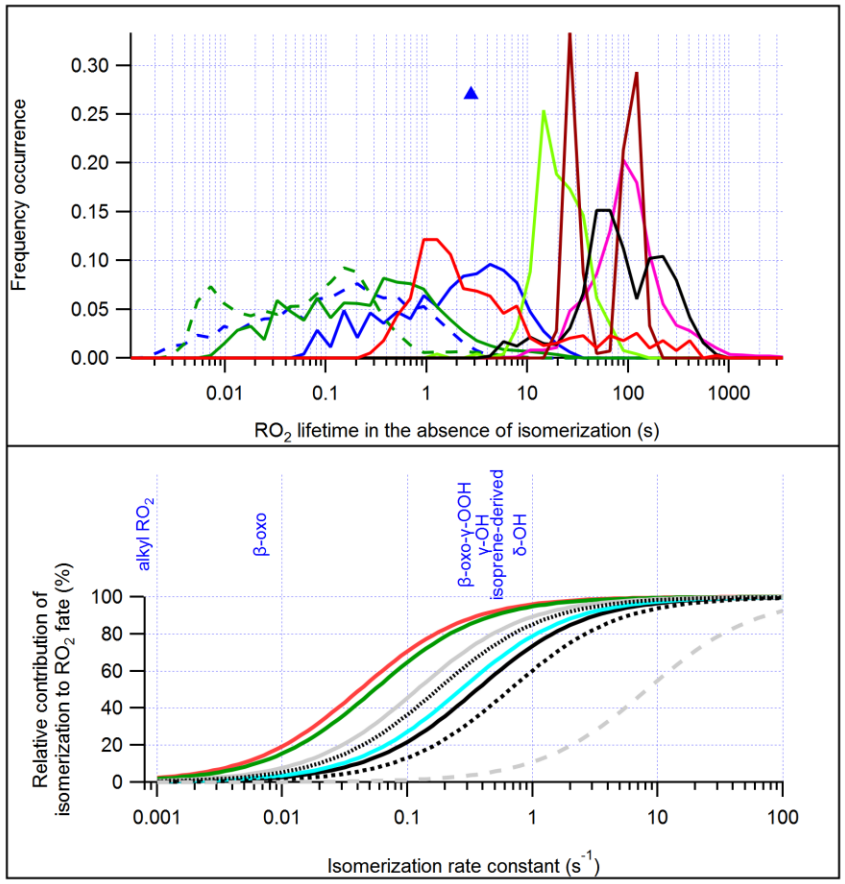

OFR185 (F185<3.16x10^{12} photons cm^{-2} s^{-1})
OFR185 (F185≥3.16x10^{12} photons cm^{-2} s^{-1})
OFR254 (F254<5.95x10^{14} photons cm^{-2} s^{-1})
OFR254 (F254≥5.95x10^{14} photons cm^{-2} s^{-1})
ATom-1 (Northern Pacific Ocean)
BEACHON-RoMBAS (Rocky Mountains)
SOAS (Forest in Southeastern US)
CalNex-LA (Los Angeles)
Chamber (FIXCIT Exp. No. 17, high OHR_{ext}, low NO)
▲ OFR185 (BEACHON-RoMBAS, max SOA)

BEACHON OFR:
Max-SOA age (~0.7 d)
Max-SOA age, 15 K higher
Max-SOA age x1/3
Max-SOA age x3
Highest UV (age of 4 mo)

Other cases:
Chamber (FIXCIT, Exp. no. 17)
Ambient (BEACHON)
Ambient (Los Angeles)

Markers:
T RO_2 isomerization rate constants

Figure 6. (top) Same format as Fig. 5, but for RO_2 lifetime (RO_2 isomerization included in the model but excluded from lifetime calculation). (bottom) Relative contribution of isomerization to RO_2 fate as a function of RO_2 isomerization rate constant in several model cases for OFR experiments in the BEACHON-RoMBAS campaign (Palm et al., 2016), in a chamber experiment and in two ambient cases. Isomerization rate constants of several RO_2 (Crounse et al., 2013; Praske et al., 2018) are also shown.

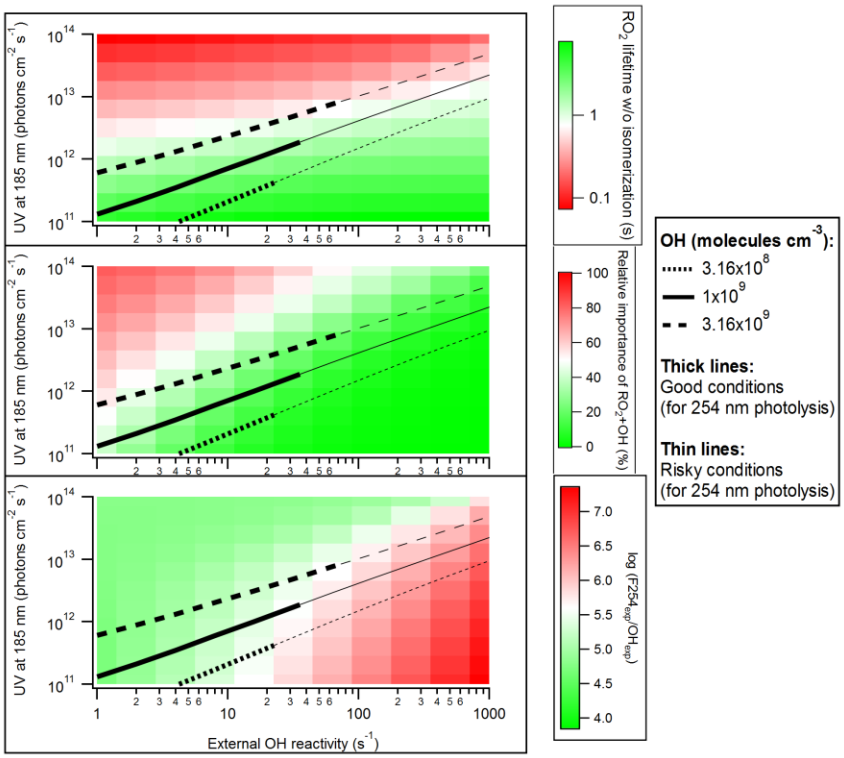

Figure 7. (top) RO_2 lifetime in the absence of isomerization, (middle) relative importance of RO_2+OH in RO_2 fate and (bottom) logarithm of the exposure ratio between 254 nm photon flux and OH as a function of 185 nm photon flux and external OH reactivity for OFR185 at N_2O=0 and H_2O=2.3%. Three lines denoting conditions leading to OH of 3.16x10^8, 1x10^9 and 3.16x10^9 molecules cm^{-3}, respectively, are added in each panel. The thick and thin parts of these lines correspond to good and risky conditions (in terms of 254 nm organic photolysis (which is usually worse than 185 nm organic photolysis; Peng et al., 2016) respectively.

Table 1. Rate constants [in cm^3 $molecule^{-1}$ s^{-1} except for isomerization (in s^{-1})] / cross section (in cm^2) and product(s) of RO_2 loss pathways. Only organic species are listed for product(s).

RO_2 loss pathway	Rate constant /cross section	Product(s)
RO_2+HO_2	$1.5x10^{-11}$ [a]	mainly ROOH for most RO_2[a]
RO_2+NO	$9x10^{-12}$ [a]	RO, $RONO_2$[b]
RO_2+RO_2	Primary: ~10^{-13} [a] Secondary: ~10^{-15} [a] Tertiary: ~10^{-17} [a] Substituted: can be up to 2 orders of magnitude higher[b] Acyl: ~10^{-11} [b]	ROH+R(=O), RO+RO, ROOR[a]
RO_2+NO_2 (in OFRs)	$7x10^{-12}$ [c]	RO_2NO_2[b]
RO_2+OH	$1x10^{-10}$ [d]	ROOOH (for ≥C4 RO_2), RO (smaller RO_2)[e]
RO_2 isomerization	Autoxidation: ~10^{-3}–10^{2} [f] Other: up to 10^{6} [g]	generally another RO_2
RO_2 photolysis	~10^{-18} at 254 nm[h] ~10^{-21}–10^{-19} in UVA and UVB[h]	mainly R, other photochemical products possible[i]
RO_2+NO_3	~1–3 $x10^{-12}$ [b]	RO[b]
RO_2+O_3	~10^{-17} [b]	RO[b]

[a]: Ziemann and Atkinson (2012);
[b]: Orlando and Tyndall (2012);
[c]: typical value within the reported range in Orlando and Tyndall (2012); thermal decomposition rate constants of nitrates of acyl and non-acyl RO_2 are assumed to be 0.0004 and 3 s^{-1}, respectively, also typical values within the reported ranges in Orlando and Tyndall (2012);
[d]: value used in the present work based on Bossolasco et al. (2014); Assaf et al. (2016, 2017a); Müller et al. (2016); Yan et al. (2016);
[e]: Müller et al. (2016); Yan et al. (2016); Assaf et al. (2017b, 2018);
[f]: Crounse et al. (2013);
[g]: Knap and Jørgensen (2017);
[h]: Burkholder et al. (2015);
[i]: Klems et al. (2015).

Table 2. Several typical ambient and chamber (the FIXCIT campaign) cases that are compared to OFR cases.

Type	Label	Case	OHR_{VOC} (s^{-1})	OH	NO	HO_2
Ambient	P_1	Pristine (Pacific Ocean, high RO_2)[a]	1.9	0.39 ppt	1.9 ppt	11 ppt
	P_2	Pristine (Pacific Ocean, typical)[a]	1	0.25 ppt	3 ppt	25 ppt
	F_1	Forested (Rocky Mountains)[b]	N/A[c]	1 ppt	60 ppt	100 ppt
	F_2	Forested (Amazon, wet season)[d]	9.6	$1.2x10^6$ molecules cm^{-3}	37 ppt	$5.1x10^8$ molecules cm^{-3}
	U	Urban (Los Angeles)[e]	25[f]	$1.5x10^6$ molecules cm^{-3} [g]	1.5 ppb[i]	$1.5x10^8$ molecules cm^{-3} [g]
Chamber (FIXCIT)	C_1	Exp. No. 25[h]	30.5[i]	$3x10^6$ molecules cm^{-3}	15 ppt	150 ppt
	C_2	Exp. No. 17[h]	116[i]	$1.2x10^6$ molecules cm^{-3}	10 ppt	50 ppt
	C_3	Exp. No. 26[h]	32[i]	$2x10^7$ molecules cm^{-3}	3.5 ppb	230 ppt
	C_4	Exp. No. 22[h]	147[i]	$2.3x10^6$ molecules cm^{-3}	430 ppb	4.3 ppb
	C_5	Exp. No. 16[h]	45.7[i]	$4x10^6$ molecules cm^{-3}	80 ppt	8 ppt

[a]: Wofsy et al. (2018) for the Atom-1 Campaign;
[b]: Fry et al. (2013), for the BEACHON-RoMBAS campaign;
[c]: RO_2 concentration was given in Fry et al. (2013) (50 ppt), so that OHR_{VOC} is not needed for RO_2 fate estimation;
[d]: personal communication from Daun Jeong and Saewung Kim for the GoAmazon Campaign (Martin et al., 2016, 2017);
[e]: typical case in the CalNex-LA campaign (Ryerson et al., 2013);
[f]: estimated (Peng et al., 2016);
[g]: typical ambient value (Mao et al., 2009; Stone et al., 2012);
[h]: data from Nguyen et al. (2014);
[i]: initial value.